UNIVERSITY OF CALGARY

A Novel Chaotic Estimation Technique and its Application to Spread Spectrum Communications

by

Haiyang Yu

A THESIS

SUBMITTED TO THE FACULTY OF GRADUATE STUDIES

IN PARTIAL FULFILMENT OF THE REQUIREMENTS FOR THE DEGREE

OF MASTER OF SCIENCE

DEPARTMENT OF ELECTRICAL AND COMPUTER ENGINEERING

CALGARY, ALBERTA

September, 2001

ABSTRACT

This thesis proposes a novel technique for estimating parameters of a noisy chaotic signal. By exploiting the ergodic property of a chaotic signal, the proposed technique is capable of estimating chaotic parameters efficiently in low signal-to-noise ratio (SNR). Simulations confirm that the proposed method outperforms other conventional chaotic parameter estimation techniques. Applying it to demodulator design for chaotic parameter modulation (CPM) spread spectrum (SS) digital communication, the new ergodic CPM (ECPM) system is shown to overcome the major handicap of current chaotic communication methods, that is, poor performance in noisy environments. The performances of ECPM and other major chaos based digital communication schemes are compared thoroughly in terms of noise performance, the effect of data rate, synchronization error and multipath channel. ECPM is found to have great performance and strong robustness under various conditions. The application of ECPM to SS analog communication is also investigated.

ACKNOWLEDGEMENTS

The author wishes to thank Dr. H. Leung sincerely, for his guidance, advice, patience and encouragement throughout the course of this work, and for his constructive criticism offered during the writing of this thesis.

The author wishes to thank the persons working in the Multimedia Signal Processing Laboratory. The author has a wonderful collaborating experience with V. Varadan, N. Xie, and S. Chan during the whole research process. The assistance of K. Murali, Y. Xia and W. Li is also greatly appreciated.

Finally, the author wishes to thank all the staff within the Department of Electrical and Computer Engineering for their support and assistance.

To Lala-

my dear wife

And

my mother and father

TABLE OF CONTENTS

Approval page.....ii

Abstract.....iii

Acknowledgements.....iv

Dedication.....v

Table of Contents.....vi

List of Tables.....viii

List of Figures.....ix

List of Abbreviations.....xiii

1. INTRODUCTION.....1

2. OVERVIEW OF CURRENT SS DIGITAL COMMUNICATION SYSTEMS BASED ON CHAOS.....7

2.1 Category I.....7

2.1.1 Chaotic spreading sequence.....7

2.1.2 Chaotic carrier.....8

2.1.3 Frequency-modulated differential chaotic shift keying.....8

2.1.4 Chaotic masking.....9

2.2 Category II.....10

2.2.1 Coherent chaotic shift keying.....10

2.2.2 Non-coherent chaotic shift keying.....11

2.3 Category III.....12

2.3.1 Chaotic parameter modulation.....12

3. NOVEL PARAMETER ESTIMATION METHOD WITH APPLICATIONS TO CPM COMMUNICATIONS.....13

3.1 Chaotic parameter estimation using the mean value method.....13

3.2 Performance evaluation of the mean value method.....17

3.3 Applications to SS digital communication system.....27

4. COMPARATIVE EVALUATION OF CHAOS BASED SS COMMUNICATION SYSTEMS WITH VARIOUS CONDITIONS.....35

4.1 Chaotic SS digital communication platform.....35

4.2 Noise performance in an AWGN channel.....37

4.3 Effect of higher transmission data rate.....42

4.4 Effect of synchronization error.....48

4.5 Multipath channels.....53

5. APPLICATION OF ECPM TO SS ANALOG COMMUNICATIONS.....59

5.1 Introduction.....59

5.2 System structure of analog ECPM scheme.....60

5.3 Performance evaluation.....62

5.4 Comparison with conventional SS digital communication systems.....70

6. CONCLUSIONS.....77

REFERENCES.....79

List of Tables

1.1. Classification of chaos based modulation schemes.....4

List of Figures

1.1. Model of DSSS digital communication system.....1

1.2. Interference rejection.....2

1.3. General system structure of chaotic SS digital communication scheme.....3

3.1. The mean value function $M(\theta)$ of the Tent map.....19

3.2. The mean value function $M(\theta)$ of the Chebyshev map.....19

3.3. The unimodal optimization function $D(\theta)$ for the Tent map with θ_0=1.3.....20

3.4. The unimodal optimization function $D(\theta)$ for the Chebyshev map with θ_0=1.65.....20

3.5. Asymptotic estimation performance of the Tent map with various sample numbers for estimation without measurement noise.....21

3.6. Asymptotic estimation performance of the Tent map versus the number of sample points and the variance of AWGN. The average power of the chaotic signal is assumed to be unity.....21

3.7. Asymptotic estimation performance of the Chebyshev map with various sample numbers for estimation without measurement noise.....22

3.8. Asymptotic estimation performance of the Chebyshev map versus the number of sample points and the variance of AWGN. The average power of the chaotic signal is assumed to be unity.....22

3.9. Performance evaluations of various parameter estimation methods for the Tent map under AWGN with exact zero mean. The parameter θ_0 is selected randomly on [1.1, 1.5].....25

3.10. Performance evaluations of various parameter estimation methods for the Chebyshev map under AWGN with exact zero mean. The parameter θ_0 is selected randomly on [1.3, 2].....25

3.11. Performance evaluations of various parameter estimation methods for the Tent map under AWGN with non-exact zero mean. The parameter θ_0 is selected randomly on [1.1, 1.5].....26

3.12. Performance evaluations of various parameter estimation methods for the Chebyshev map under AWGN with non-exact zero mean. The parameter θ_0 is selected randomly on [1.3, 2]....26
3.13. Block diagram of ergodic chaotic parameter modulation (ECPM) communication system....28
3.14. Detailed simulation model of the proposed ergodic chaotic parameter modulation (ECPM) system based on the Chebyshev map for SS digital communications....28
3.15. Signal waveforms in various stages of the ECPM communication system....31
3.16. The time waveform and power spectrum density of the original binary message and modulated chaotic signal....31
3.17. Comparison of the BER performance of various CPM systems in AWGN channel with exact zero mean noise....33
3.18. Comparison of the BER performance of various CPM systems in AWGN channel with the noise mean is not exactly zero....34
4.1. Phase space portrait of the Chebyshev map with $\theta = 2$....36
4.2. Noise performance of the different chaos based schemes in an AWGN channel....38
4.3. Autocorrelation function of (a) the spreading sequence for the CSS approach and (b) the chaotic carrier for the CC method....39
4.4. The histogram plots of the output signals of the demodulator of (a) ECPM and (b) FM-DCSK in a noise free environment, and (c) ECPM and (d) FM-DCSK in the noise environment of $E_bNR = 10\ dB$ 40
4.5. Synchronization performance of the chaotic synchronization system under the noise free condition. (a) The transmitted and recovered chaotic signals and (b) the synchronization error....42
4.6. Model of the transmitted signal with higher transmission data rate....43
4.7 Noise performance of various chaos based scheme with data rate is $f_b = 500\ kbps$ 44
4.8. Noise performance of various chaos based scheme with data rate is

f_b = 1 Mbps.....44
4.9. Histogram plots of the observed bit energies at the output of the demodulator of NCSK in a noise free environment with (a) T_b = 2 μs, and (b) T_b = 1 μs.....45
4.10. Performance analysis of the chaotic parameter tracking based on the gradient search method for SNR ≈ 20 dB. (a) The convergence of the chaotic parameter of the Chebyshev map and (b) the corresponding tracking error.....46
4.11. Noise performance of ECPM with different data rate f_b = 50 kbps, f_b = 500 kbps and f_b= 1 Mbps separately.....47
4.12. The channel model of the non-ideal system with propagation delay of the received signal passed through an AWGN channel.....49
4.13. The distribution plot of the propagation delay within each bit duration T_b.....50
4.14. Effect of synchronization error on the various chaos based communication systems.....50
4.15. Performance of FM-DCSK through propagation delay channel with different delay ranges.....52
4.16. Propagation delay model of a multipath channel with additive white Gaussian noise.....54
4.17. Multipath intensity profile illustration for different propagation delays paths.....55
4.18. BER performance of the different chaos based communication systems in a multipath channel.....56
5.1 Block diagram of the demodulator of the analog ECPM system 60
5.2 Detailed structure of the simulation model of analog ECPM system.....63
5.3 Signal waveforms in various stages of the proposed ECPM SS analog communication system.....65
5.4. Recovery performance for sinusoidal signal and Gaussian random signal.....66
5.5. Recovery performance of the speech signal through the proposed ECPM

SS analog communication system. SNR = 0 dB, processing gain G = 1000, recover quality MSE = -25.657 dB.....68

5.6. Recovery performance of the image signal through the proposed ECPM SS analog communication system, SNR = 0 dB, processing gain G = 1000, recover distortion MSE = -29.448dB.....69

5.7. Signal recovery performance for speech and image signals.....70

5.8. Comparison of analog ECPM system with conventional digital DSSS system, no error control coding is employed in the DSSS system.....72

5.9. Distortion performance of various quantization schemes for discrete-time memoryless Gaussian source.....73

5.10. Comparison of analog ECPM system with conventional digital DSSS system, BCH error control coding is employed in the DSSS system.....75

List of Abbreviations

ADC	Analog to digital conversion
ADM	Amplitude demodulation
AF-CPM	Adaptive filtering chaotic parameter modulation
AM	Amplitude modulation
AWGN	Additive white Gaussian noise
BCH	Bose-Chaudhuri-Hocquenghem codes
BER	Bit error rate
BPSK	Binary phase shift keying
CC	Chaotic carrier
CCSK	Coherent chaotic shift keying
CM	Chaotic masking
CPM	Chaotic parameter modulation
CSK	Chaotic shift keying
CSS	Chaotic spreading sequence
DAC	Digital to analog conversion
DSB-AM	Double-sideband amplitude modulation
DSSS	Direct sequence spread spectrum
E_bNR	Energy per bit to noise spectrum density ratio
ECPM	Ergodic chaotic parameter modulation
EKF	Extended Kalman filter
E_sNR	Energy per signal to noise spectrum density ratio
FM	Frequency modulation
FM-DCSK	Frequency modulated differential chaotic shift keying
LMS	Least mean square
MAP	Maximum a posteriora
ML	Maximum-likelihood
MSE	Mean square error
NCSK	Non-coherent chaotic shift keying

PN	Pseudorandom noise
QoS	Quality of service
RF	Radio frequency
RLS	Recursive least square
SNR	Signal power to noise spectrum density ratio
SS	Spread spectrum
WLAN	Wireless local area network

CHAPTER 1

INTRODUCTION

In a conventional spread spectrum (SS) digital communication system, the spreading signals used to transmit digital information are distinguished by their wideband, flat spectrum, and pseudo-randomness. Roughly speaking, a SS signal is generated by modulating a data signal onto a wideband carrier so that the resultant transmitted signal has bandwidth that is much larger than the information rate [1,2].

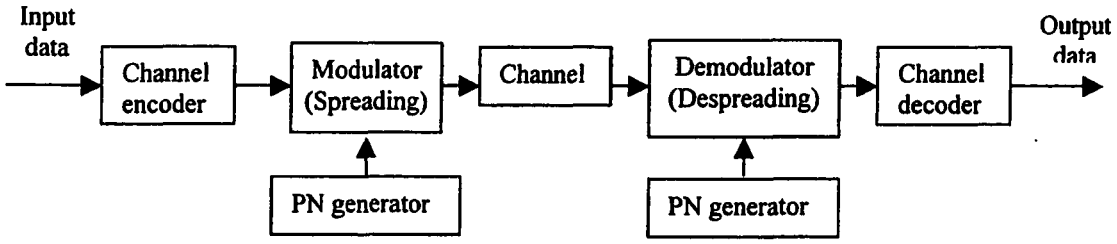

Figure 1.1. Model of DSSS digital communication system.

The block diagram shown in Figure 1.1 illustrates the basic elements of the conventional direct sequence SS (DSSS) digital communication system with a binary information sequence at its input at the transmitting end and at its output at the receiving end. The channel encoder and decoder and the modulator and demodulator are basic elements of the system. In addition to these elements, we have two identical pseudo-random pattern generators, one that interfaces with the modulator at the transmitting end and a second that interfaces with the demodulator at the receiving end. The generators generate a pseudo-noise (PN) binary-valued sequence, which is impressed on the transmitted signal at the modulator and removed from the received signal at the demodulator. Synchronization of the PN sequences generated at the receiver with the PN sequences contained in the incoming received signal is required in order to demodulate the received signal. Initially, prior to the transmission of information, synchronization may be achieved by transmitting a fixed pseudo-random bit pattern that the receiver will recognize in the presence of interference with a high probability. After time

synchronization of the generators is established, the transmission of information may commence.

The expanding bandwidth of the signal could overcome the severe levels of interference that are encountered in the transmission of digital information. This is illustrated in Figure 1.2. The spread spectrum signal, *s,* receives a narrowband interference, *i.* At the receiver end, the SS signal is "despread" while the interference signal is spread, making it appear as background noise compared to the despread signal. The pseudo-randomness of SS signal makes it appear similar to random noise. It follows that its pseudo-randomness could make the signal less detectable.

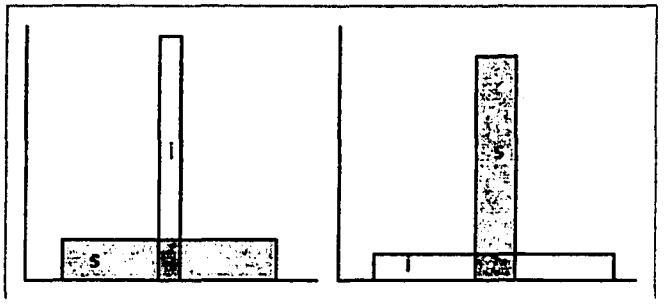

Figure 1.2. Interference rejection.

The SS techniques have been successfully used in many practical communication fields [3]. As we know, in order to design a spread spectrum scheme, it is necessary that the transmitted signal of the system must satisfy two criteria. First, the bandwidth of the transmitted signal must be much greater than the message bandwidth. Second, the transmitted bandwidth must be determined by some function that is independent of the message. Recently, application of chaos to SS communications has drawn a great deal of attention. Chaos is quite suitable for a spread spectrum communication system because (i) the chaotic signal is broadband signal in nature, which has much greater bandwidth than the information bandwidth; (ii) the non-linear chaotic signal is completely independent of the information signal.

A chaotic system is a non-linear deterministic dynamical system whose states change with time in a deterministic way [4,5]. For a discrete time chaotic system, the state equation can be expressed as:

$$x(t) = f(\mathbf{x}(t-1), \theta), \tag{1.1}$$

where $\mathbf{x}(t-1)=[x(t-1), x(t-2), \cdots, x(t-d)]^{\mathrm{T}}$ is the d-dimensional state vector at time t-1, and f is the non-linear state function, and θ is the bifurcating parameter lying in the chaotic regime $[\theta_{min}, \theta_{max}]$.

Application of chaos to communications has been found to offer many advantages to the conventional SS system including security, hardware implementation, synchronization and potential for performance enhancement [6]. Various chaotic communication schemes have been proposed in the literature [7-9]. Figure 1.3 gives the general structure of a chaotic SS communication system. The only difference between the conventional DSSS system shown in Figure 1.1 and the chaotic SS system is the application of chaotic modulation (spreading) and chaotic demodulation (despreading) techniques. These approaches exploit different characteristics of a chaotic system to achieve SS communication.

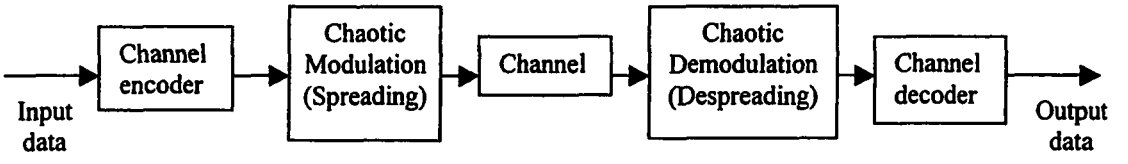

Figure 1.3. General system structure of chaotic SS digital communication scheme.

Based on the different ways of modulating the digital information, we classify the current chaos based SS schemes into three major categories as shown in Table 1.1. From the chaotic equation (1), there are three intuitive variables: the chaotic state $x(t)$, the nonlinear map f, and the bifurcating parameter θ. The chaotic communication schemes are categorized according to these three variables. First, the digital information is modulated by using the chaotic states $x(t)$. It means that the chaotic signal generated from a chaos system is served as the modulation carrier directly. $x(t)$ can be used to mask the information signal or be used to generate binary spreading codes. Chaotic communication schemes including chaotic spread sequence (CSS) [10-12], chaotic carrier (CC) [13,14], frequency-modulated differential chaotic shift keying (FM-DCSK) [15,16] and chaotic masking (CM) [17,18] all belong to this category. Second, the digital information is modulated into the chaos system by using the chaotic state function f. For instance, in a chaos shift keying (CSK) system, different chaotic state functions are used to represent

different digital states. Demodulating the digital information is then equivalent to determining which state function is used to generate the transmitted chaotic signal [19-21]. Third, the digital information is modulated by emerging it into the chaotic bifurcating parameter θ. By controlling the parameter θ in an appropriate chaotic regime, the information signal will be carried by the chaotic signal for SS transmission. At the receiver, the demodulation is then a parameter estimation process, and this scheme is called chaotic parameter modulation (CPM) [22,23].

	Category I: Chaotic states $x(t)$	Category II: Chaotic state function f	Category III: Bifurcating parameter θ
Modulation method	Modulating with the chaotic signal	Modifying the state function	Controlling the parameter
Demodulation method	Retrieve the digital information out from the chaotic signal	Determination of the state function used for the transmitted chaotic signal	Tracking the parameter used for the transmitted chaotic signal
Schemes	CSS, CC, FM-DCSK, CM	CSK	CPM

Table 1.1. Classification of chaos based modulation schemes

There are many active ongoing researches have been carrying out for these chaotic communication schemes. CPM is one of the most interesting chaotic communication schemes, which employs a chaotic dynamical system to modulate the signal of transmission to achieve the goal of SS communications for both digital and analog transmission. The CPM scheme is not only theoretically interesting, but also offers many advantages to the conventional SS systems. Compared to conventional SS approaches based on spreading codes, the CPM scheme does not require the complicated synchronization procedure for demodulation and has the potential of higher system capacity. However, the CPM scheme needs a demodulator that can estimate the parameter of a chaotic signal accurately to demodulate the message signal. When

measurement noise exists, many conventional estimators are found not working efficiently. Their estimation performances are not good enough to build a practical communication system [9, 22] and cannot guarantee a reliable communication. Therefore, a new chaotic estimator is necessary to be developed.

The problem of chaotic estimation has been investigated by some researchers and can be classified into two major categories: estimating a signal in chaotic noise and estimating a chaotic signal in random noise. Mathematically, given a received signal $r(t) = x_\theta(t) + n(t)$, the problem of chaotic estimation occurs when either *n(t)* or *x(t)* is chaotic. The former problem is found in situations where the background noise is chaotic such as signal estimation in radar clutter [24], de-reverberation of room acoustics [25] and blind channel equalization and interference cancellation for chaotic communications [26,27]. The latter chaotic estimation problem is closely related to noise filtering [28] and signal reconstruction [29]. For the many applications of the latter estimation problem, the functional form of *x(t)* is usually given and hence we only need to estimate the unknown parameters of the signal *x(t)*. There are two parameters in *x(t)* that are usually of interest to us, i.e. the initial condition and the bifurcating parameter θ. The chaotic estimation problem has been studied by several researchers. Some of these techniques have shown to have good performances but only at high signal to noise ratios (SNR) [30,31,32].

In this thesis, we propose a novel technique, called mean value method, for estimating the bifurcating parameter of a chaotic signal at low SNR based on the Birkhoff ergodic theorem for dynamical systems. We show here that the chaotic parameters can be estimated accurately even the background noise is very strong. By applying this estimation scheme to the CPM communication scheme, we found that the performance of the SS CPM digital communication system has been well improved. This new communication scheme called ergodic CPM (ECPM) can operate in various communication conditions. Its performance is compared to other major chaos based SS communication systems according to the noise performance, robustness to synchronization error, capacity for high data rate transmission and immunity for the multi-path effect. These factors are chosen since they are fundamental elements for designing a practical SS communication system. Further more, by applying the mean

value method as the demodulator, the ECPM system can be also implemented for analog SS transmission. This ECPM analog communication system is the only SS approach based on analog formats to-date to the best of our knowledge.

Since one-dimensional chaotic systems are of particular interest due to their potential applications in many areas such as pattern recognition [33], SS communications [6], secure communication [34] and coding [35] and the fact that many signal processing techniques have been devoted to one-dimensional chaotic signals [36], our presentation here is mainly focused on one-dimensional chaotic systems for a more rigorous formulation. The thesis is organized as follows. Chapter 2 gives a brief overview of all chaos based SS digital communication schemes. In Chapter 3, the basic idea of the proposed chaotic parameter estimation based on ergodic theory is described. Theoretical analysis and simulation results of this estimation method are also given. By applying this technique as the demodulator of the CPM system, the performance of this digital scheme, so called ECPM, is compared with the conventional CPM communication system. Chapter 4 presents a simulation platform to perform comparative evaluations of the proposed digital ECPM scheme with other major chaos based communication schemes. The noise performance, effect of high transmission data rate, synchronization error and multipath channel are investigated. In Chapter 5, the application of ECPM to the SS analog transmission is addressed. Its performance is evaluated by transmitting various kinds of analog signals. The performances of this analog ECPM and the conventional DSSS digital systems are also compared. Concluding remarks are given in Chapter 6.

CHAPTER 2

OVERVIEW OF CURRENT SS DIGITAL COMMUNICATION SYSTEMS BASED ON CHAOS

In this section, various major chaos based SS communication systems are briefly overviewed. The readers are referred to the references for the details. The following symbols are used in our presentation. $x(t)$ denotes the chaotic signal generated from a chaotic state function f as shown in (1.1); θ denotes the chaotic bifurcating parameter; $x'(t)$ represents the modulated signal; $n(t)$ denotes the channel noise; $d(n)$ represents the binary information data; T_b is the bit duration and $m(n)$ denotes the sampled output of a demodulator.

2.1 Category I

2.1.1 Chaotic spreading sequences

In a direct sequence SS (DSSS) communication system, uncorrelated binary pseudo-random (PN) sequences with good auto-correlation and cross-correlation properties, such as Gold sequences and Kasami sequences are used as spreading codes [1]. The noise-like behavior of a PN sequence stimulates the use of chaotic signal for spreading sequences [37,38]. Given a chaotic system as shown in (1.1), a binary chaotic spreading sequence $b(k)$ can be obtained from the chaotic signal $x(t)$ by using the following mapping:

$$b(k) = g\left(x(t) - E\left[x(t)\right]\right)_{t=kT_x}, \tag{2.1}$$

where $g(x)=1$ for $x \geq 0$ and $g(x)=0$ for $x<0$, $\mathrm{E}[x(t)]$ is the expectation of $x(t)$, and T_x is the discrete sampling duration of $x(t)$. In a DSSS system, T_x is viewed as the chip duration. At the receiver side, an identical synchronized chaotic system is employed to generate the chaotic spreading signal. A coherent correlator is usually employed to demodulate the transmitted signal. This chaotic communication approach is basically the same as the conventional DSSS system except that the spreading code is generated by a chaotic

system. The difference in the performance of the CSS scheme therefore mainly comes from the difference in the correlation of the spreading codes.

2.1.2 Chaotic carrier

Chaotic carrier (CC) is another direct application of a chaotic signal to a conventional SS communication system by using the chaotic signal as the transmitted carrier directly [13, 14]. The suggested chaotic carrier $x'(t)$ is given by [13]

$$x'(t)=\sum_{i=1}^{N} x_i(t)\cos(\omega_c t+\varphi_i), \quad N\in[1,\infty), \tag{2.2}$$

where ω_c is the central frequency of the transmission carrier, φ_i is a random variable uniformly distributed on $(-\pi,\pi]$. The chaotic carrier can be the chaotic signal generated from only one chaotic system ($N = 1$), or can be the combination of the chaotic signals generated from multiple chaotic systems ($N > 1$). According to (2.2), the chaotic carrier can be generated unlimitedly and non-periodically.

In this CC modulation scheme, the digital message is modulated by an analog chaotic carrier rather than a binary sequence as in the CSS scheme. Because a chaotic signal has an auto-correlation close to delta function, at the receiver side, the transmitted binary information of this CC scheme can be retrieved by applying a correlator and a threshold detector.

2.1.3 Frequency-modulated differential chaotic shift keying

One of the most popular chaotic communication schemes to-date is the frequency-modulated differential chaotic shift keying (FM-DCSK) modulation [15,16]. The basic concept of a FM-DCSK system is that every binary information bit *d(n)* is mapped to two chaotic sample functions, while the first function is used as a reference, the second one represents the information to be transmitted. When the data "0" is to be transmitted, the reference signal *x(t)* generated from the chaotic system is transmitted within the first half bit duration [0, $T_b/2$]. After that, the chaotic signal *x(t)* is used again for transmission in the second half bit duration [$T_b/2$, T_b]. When the data "1" is to be transmitted, *x(t)* is transmitted in the first half bit duration but its negative waveform is used instead in the second half bit duration. That is,

$$x'(t)=\begin{cases}\begin{cases} x(t), & 0\le t<T_b/2 \\ x(t-T_b/2), & T_b/2\le t<T_b; \end{cases} & d(n)=0 \\ \begin{cases} x(t), & 0\le t<T_b/2 \\ -x(t-T_b/2), & T_b/2\le t<T_b. \end{cases} & d(n)=1. \end{cases} \tag{2.3}$$

At the receiver side, a self-synchronized correlator is employed where the received signal within the time period of $[0,T_b/2]$ is multiplied with the signal within time period of $[T_b/2,T_b]$. The sampled output of the correlator can be expressed as

$$m(n)=\int_{T_b/2}[x'(t)+n(t)]\cdot[(x'(t-\frac{T_b}{2})+n(t-\frac{T_b}{2})]dt\,. \tag{2.4}$$

According to the differential modulation rules, a positive correlation between the signals within the first half bit duration and the second half bit duration indicates that a "0" is received. On the other hand, when a negative correlation is found, it means the reception of the data "1". The decision is made by a simple level comparator, which has a constant, zero threshold level, as shown below

$$\hat{d}(n)=\begin{cases}0 & m(n)\ge 0 \\ 1 & m(n)<0\end{cases}. \tag{2.5}$$

2.1.4 Chaotic masking

The chaotic masking (CM) is originally proposed for transmitting analog signals. The analog information is directly added to a wide-band chaotic signal for transmission [17,18]. Based on the capability of chaotic synchronization [21,39], the chaotically masked signal is used at the receiving end to drive the chaotic synchronization system. By subtracting the reconstructed chaotic signal $x_r(t)$ from the received signal, the transmitted information signal can then be determined. The CM communication scheme can also be applied to a digital signal $d(n)$ as shown below:

$$x'(t)=\begin{cases}x(t)+A, & if \quad d(n)=1; \\ x(t)-A, & if \quad d(n)=0\end{cases} \tag{2.6}$$

where A is the added information level. The demodulation process is therefore required to remove the channel noise as well as the masking chaotic signal. A widely used demodulator for a digital CM scheme is given by

$$m(n) = \frac{1}{T_b}\int_0^{T_b}\{x'(t) + n(t) - x_r(t)\}dt$$
$$= \frac{1}{T_b}\int_0^{T_b}\{x(t) \pm A + n(t) - x_r(t)\}dt \quad (2.7)$$

If chaotic synchronization is performed successfully, the reconstructed chaotic signal $x_r(t)$ will be identical to the transmitted chaotic signal, $x_r(t) \approx x(t)$. Thus the masked chaotic signal can be removed. Noted that $\frac{1}{T_b}\int_0^{T_b} n(t)dt \approx 0$ if $n(t)$ is AWGN process, the decision can be made by setting a zero threshold level as shown below:

$$\hat{d}(n) = \begin{cases} 1 & m(n) \geq 0 \\ 0 & m(n) < 0 \end{cases} \quad (2.8)$$

2.2 Category II

Chaotic shift keying (CSK) uses different state equations of chaotic systems to represent the different information symbols for transmission [19]. More precisely, each the binary symbols "0" and "1" are assigned to different chaotic maps f_i, $i = 0, 1$ by the following rules:

$$x'(t) = \begin{cases} x_0(t) \text{ for } d(n) = 0 \text{ where } x_0(t) = x(t) \text{ and } x(t) = f_0(x(t-1)) \\ x_1(t) \text{ for } d(n) = 1 \text{ where } x_1(t) = x(t) \text{ and } x(t) = f_1(x(t-1)) \end{cases} \quad (2.9)$$

The demodulator is therefore to decide, on the basis of a received noisy and distorted sample function, which map is more likely to have been used in producing the received waveform. Two different demodulators for CSK have been proposed in the literature [8]: the coherent CSK (CCSK) which is based on the synchronized chaotic synchronization and the non-coherent CSK (NCSK) which uses the self-correlator to demodulate the transmitted data.

2.2.1 Coherent chaotic shift keying

Two chaotic synchronization systems are installed at the receiver corresponding to the two chaotic maps f_i, $i = 0, 1$ used in the transmitter. The received signal is used as a driving signal to both synchronization systems. The reconstructed signals from both synchronization systems are operated with the received signal to perform correlation function. That is,

$$\begin{cases} m_0(n) = \int_{T_b}(x'(t)+n(t))\cdot x_{r0}(t)dt = \int_{T_b}x'(t)x_{r0}(t)dt + \int_{T_b}x_{r0}(t)n(t)dt \\ m_1(n) = \int_{T_b}(x'(t)+n(t))\cdot x_{r1}(t)dt = \int_{T_b}x'(t)x_{r1}(t)dt + \int_{T_b}x_{r1}(t)n(t)dt, \end{cases} \tag{2.10}$$

where $x_{r,i}(t)$ is the reconstructed chaotic signal for the chaotic map f_i. Comparing the outputs of the two correlators, the largest one is selected and hence the transmitted binary data is decided. That is,

$$\hat{d}(n) = \begin{cases} 0 & m_0 > m_1 \\ 1 & m_1 \geq m_0. \end{cases} \tag{2.11}$$

Only the matched synchronization system can generate the identical signal to the transmitted chaotic signal. The signal generated from the other unmatched one is uncorrelated with the transmitted chaotic signal.

2.2.2 Non-coherent chaotic shift keying

Unlike the CCSK, the non-coherent CSK (NCSK) uses the transmitted chaotic signal itself as the reference signal to perform correlation. The output of the demodulator is given by:

$$\begin{aligned} m(n) &= \int_{T_b}(x'(t)+n(t))(x'(t)+n(t))dt \\ &= \int_{T_b}x'(t)^2dt + 2\int_{T_b}x'(t)n(t)dt + \int_{T_b}n(t)^2dt \end{aligned} \tag{2.12}$$

The decision is based on the property that the bit energies of chaotic signals from different chaotic maps are different, i.e. $\int_{T_b}x_0(t)^2dt \neq \int_{T_b}x_1(t)^2dt$. By applying a threshold to the detector in (2.12), the transmitted binary data can then be determined

$$\hat{d}(n) = \begin{cases} 0 & m(n) < Threshold \\ 1 & m(n) \geq Threshold \end{cases}, \tag{2.13}$$

where the threshold can be set as $\frac{1}{2}\left[\int_{T_b}x_0(t)^2dt + \int_{T_b}x_1(t)^2dt\right]$ by assuming $\int_{T_b}x_0(t)^2dt < \int_{T_b}x_1(t)^2dt$.

2.3 Category III

2.3.1 Chaotic parameter modulation

Chaotic parameter modulation (CPM) modulates the message signal into the parameter of a chaotic system to achieve the goal of SS communication. The message signal can be either analog or digital. For digital communication with binary data *d(n)*, CPM can be expressed as

$$x'(t)=\begin{cases} x(t)=f[x(t-1),\theta_0] & if \quad d(n)=0 \\ x(t)=f[x(t-1),\theta_1] & if \quad d(n)=1 \end{cases}, \tag{2.14}$$

where θ_0 and θ_1 are different bifurcating parameter values. The demodulation is therefore equivalent to estimating the bifurcating parameter from the chaotic signal $x'(t)$. The goal of the demodulator is to determine which parameter is used and then determine which binary data is transmitted. Currently, adaptive filtering algorithms such as least mean square (LMS), recursive least square (RLS), extended Kalman filter (EKF) have been proposed to estimate and track the chaotic parameter [22]. This kind of system is therefore called adaptive filtering chaotic parameter modulation (AF-CPM) in our study. Their tracking and estimation abilities make them suitable for demodulating the transmitted binary information in real time communication system [23]. The basic idea of these adaptive filtering algorithms is to minimize some error function such as the mean square error between the estimated and measured state values by searching for an optimal chaotic parameter. Assuming that the modulated signal is corrupted by AWGN channel noise, i.e. $r(t)=x'(t)+n(t)$, the AF-CPM demodulator based on the general gradient search method [40,41] is given by

$$\hat{\theta}_k=\hat{\theta}_{k-1}-\mu[r_k-f(r_{k-1},\hat{\theta}_{k-1})]\left.\frac{df(r,\theta)}{dr}\right|_{\substack{r=r_{k-1}\\ \theta=\hat{\theta}_{k-1}}}. \tag{2.15}$$

After the determination of the parameter $\hat{\theta}$, the decision process for the transmitted symbol can be carried out by

$$\hat{d}(n)=\begin{cases} 0 & if\ \hat{\theta}\ is\ closer\ to\ \theta_0 \\ 1 & if\ \hat{\theta}\ is\ closer\ to\ \theta_1 \end{cases}. \tag{2.16}$$

CHAPTER 3

NOVEL PARAMETER ESTIMATION METHOD WITH APPLICATIONS TO CPM COMMUNICATIONS

From the description of CPM in subsection 2.3, we can see that the parameter estimation is the most important keying consideration for the operation of the CPM system. The bifurcating parameter estimation problem will be considered in this chapter. This problem is not only of theoretical interest, but it also has many applications such as nonlinear model identification and chaotic communications. It can be directly applied to the demodulator design for CPM communications. In [22,23], adaptive filters including the least mean square (LMS), recursive least square (RLS) and extended Kalman filter (EKF) have been considered for demodulating a chaotic parameter modulated signal. However, all these adaptive filter based demodulators have relatively poor performances at low signal to noise ratio (SNR) and cannot guarantee a reliable communication. A novel technique called mean value method for estimating the parameter of a chaotic signal is proposed here. It is capable of estimating chaotic signal parameters efficiently at low signal-to-noise ratio (SNR).

3.1 Chaotic parameter estimation using the mean value method

Let f_θ be a chaotic map defined on some closed interval and the parameter θ lies between $[\theta_{min}, \theta_{max}]$. Let $x(t)$ be a chaotic signal generated by f_θ and $r(t)$ be its noisy observation. That is,

$$x(t) = f_\theta(\mathbf{x}(t-1)) \tag{3.1}$$
$$r(t) = x(t) + n(t),$$

where $\mathbf{x}(t-1) = [x(t-1), x(t-2), \cdots, x(t-d)]^T$ is the d-dimensional state vector at time $t-1$, $n(t)$ is a zero-mean AWGN process. The chaotic parameter estimation problem is then to estimate the parameter θ from the noisy observations $r(t)$.

Considering that for each $\theta \in [\theta_{min}, \theta_{max}]$, the map f_θ has a unique invariant ergodic measure μ_θ. The chaotic signal *x(t)* is basically an orbit of f_θ with the starting point *x(0)*. According to the Birkhoff ergodic theorem [4], the limit $\lim_{N\to\infty}\frac{1}{N}\sum_{t=1}^{N}x(t)$ exists and is equal to the constant $\int x d\mu_\theta(x)$. This limit is independent of the initial condition *x(0)* and depends only on the parameter θ. We call this function the mean value function $M(\theta)$ of the chaotic map f_θ. For many chaotic maps, we have an interesting observation that their mean value functions are in fact monotone. This implies that it is possible, at least in theory, to estimate a particular parameter value θ_0 by the following procedure. Assuming that *r(t)*is generated by (3.1) with $\theta = \theta_0$. First, we estimate the mean value $M_0 = M(\theta_0)$ from the received signal *r(t)*. Second, we invert the function $M(\theta)$ to obtain an estimate of θ_0, i.e. $\hat{\theta}_0 = M^{-1}(M_0) = M^{-1}(M(\theta_0))$. Since $M(\theta)$ is monotone, the existence of M^{-1} is guaranteed.

To avoid deriving the inverse mean value function M^{-1} which may be difficult to obtain analytically, we can obtain $\hat{\theta}_0$ by solving the following optimization problem. Suppose that the mean value function $M(\theta)$ is continuous and monotone on the interval $[\theta_{min}, \theta_{max}]$. If $M(\theta_0)$ is given, then θ_0 can be determined by finding the minimum of $D(\theta) = |M(\theta) - M(\theta_0)|$ for $\theta \in [\theta_{\min}, \theta_{\max}]$.

Theorem 1 If $\hat{\theta} = \min_\theta D(\theta) = \min_\theta |M(\theta) - M(\theta_0)|$, then $\hat{\theta} = \theta_0$.

Proof: Let $D(\theta) = |M(\theta) - M(\theta_0)|$, $D(\theta_0) = 0$ implies that θ_0 is a global minimum of $D(\theta)$ on the interval $[\theta_{min}, \theta_{max}]$ since $D(\theta)$ is nonnegative. Given that $M(\theta)$ is continuous and monotone, $D(\theta)$ is a continuous unimodal function on $[\theta_{min}, \theta_{max}]$ and hence θ_0 is a unique global minimum of $D(\theta)$. Therefore, finding the minimum of $D(\theta)$ is equivalent to determining θ_0.

The above theorem is rather straightforward, but it is the main concept of the proposed method. The proof is therefore given for the sake of completeness. To make this mean value concept useful for practical estimation, $M(\theta)$ and $M(\theta_0)$ should be known or

determined to have the function $D(\theta)$ for optimization. We apply the mean value limit given above to the noisy received signal to get an approximation of $M(\theta_0)$. That is,

$$\hat{M}(\theta_0) = \frac{1}{N}\sum_{t=1}^{N} r(t) = \frac{r(1)+r(2)+\cdots+r(N)}{N}. \tag{3.2}$$

Theorem 2 The mean value estimator $\hat{M}(\theta_0)$ is consistent.

Proof: According to the Birkhoff ergodic theorem for the ergodic maps f_θ and the strong law of large numbers of i.i.d. sequence, we have

$$\hat{M}(\theta_0) = \frac{1}{N}\sum_{t=1}^{N} r(t) = \frac{1}{N}\sum_{t=1}^{N} x(t) + \frac{1}{N}\sum_{t=1}^{N} n(t). \tag{3.3}$$

Let $\hat{M}_1(\theta_0) = \frac{1}{N}\sum_{t=1}^{N} x(t)$ and $\hat{M}_2 = \frac{1}{N}\sum_{t=1}^{N} n(t)$, then $\hat{M}(\theta_0) = \hat{M}_1(\theta_0) + \hat{M}_2$. Since f_θ is ergodic, $\hat{M}_1(\theta_0)$ approaches $M(\theta_0)$ as N approaches infinity. Similarly, if *n(t)* is a white Gaussian process, by the strong law of large numbers, $\hat{M}_2$ approaches zero since $\hat{M}_2$ is a consistent estimator of the mean of the white Gaussian noise process. Therefore $\hat{M}(\theta_0)$ is a consistent estimator of $M(\theta_0)$ and consequently the estimator $\hat{\theta}_0$ is also a consistent estimator of θ_0.

Not only can we prove that the mean value estimator $\hat{M}(\theta_0)$ is consistent, but the asymptotic variance can also be derived analytically as shown in the following theorem.

Theorem 3 The asymptotic variance of the estimator $\hat{M}(\theta_0)$ is equal to $\frac{\sigma_1^2+\sigma_2^2}{N}$ and the asymptotic variance of the estimate $\hat{\theta}_0$ is equal to $(M^{-1}(M(\theta_0)))^2 \frac{\sigma_1^2+\sigma_2^2}{N}$, where N is the number of sample points in the noisy chaotic signal, σ_1^2 is the chaotic signal power and σ_2^2 is the noise power.

Proof: According to the Central Limit Theorem for Markov maps [42], the variable $\frac{1}{\sigma_1\sqrt{N}}\sum_{j=0}^{N-1}[x(j) - M(\theta_0)]$ converges in distribution to the standard unit normal random variable. Here σ_1 is defined by $\sigma_1^2 = R(0) + 2\sum_{t=1}^{\infty} R(t)$, where *R(t)* denotes the

autocovariance sequence of the chaotic signal *x(t)*. This implies that the random variable $\frac{\hat{M}_1(\theta_0) - M(\theta_0)}{\sigma_1 / \sqrt{N}}$ converges in distribution to the standard unit random variable. Similarly, by the Central Limit Theorem for i.i.d. sequences, the random variable $\frac{\hat{M}_2}{\sigma_2 / \sqrt{N}}$ converges in distribution to the standard unit normal random variable where σ_2^2 denotes the variance of the additive white Gaussian noise. Since $\hat{M}_1(\theta_0)$ and $\hat{M}_2$ are independent, $\frac{(\hat{M}_1(\theta_0) - M(\theta_0)) + \hat{M}_2}{\sqrt{(\sigma_1^2 + \sigma_2^2)/N}}$ converges to the standard unit normal random variable. Therefore, the asymptotic variance of the consistent estimator $\hat{M}(\theta_0)$ is equal to $\frac{\sigma_1^2 + \sigma_2^2}{N}$. Assuming that the mean value function $M(\theta)$ is smooth and monotone, there exists a smooth inverse function M^{-1}. Since $\hat{\theta}_0 = M^{-1}(\hat{M}(\theta_0))$, the asymptotic variance of $\hat{\theta}_0$ is equal to

$$(M^{-1}(M(\theta_0)))^2 \frac{\sigma_1^2 + \sigma_2^2}{N}, \tag{3.4}$$

where σ_1^2 and σ_2^2 are the chaotic signal power and the noise power respectively.

Although $\hat{M}(\theta_0)$ can be computed easily from the received signal *r(t)* using the ensemble average, we still need to find the mean value function $M(\theta)$ to perform the optimization on $D(\theta)$. Unfortunately, derivation of $M(\theta)$ is not entirely easy and in fact there may not be a closed form expression of the mean value function for all chaotic maps. Since we can obtain an accurate estimate of $M(\theta_i)$ for any $\theta_i \in [\theta_{\min}, \theta_{\max}]$ using the ensemble average, the value of $M(\theta)$ can be computed numerically with high accuracy for any θ. We therefore propose using some numerical technique such as the Golden section search method to locate the minimum of $D(\theta)$ on $[\theta_{min}, \theta_{max}]$ and hence obtain the estimate $\hat{\theta}_0$.

The mean value estimation algorithm is summarized as follows:

1. Compute an estimate of the mean value of the received signal *r(t)* using the ensemble average, that is, $\hat{M}(\theta_0) = \frac{r(1)+r(2)+\cdots+r(N)}{N} = \frac{1}{N}\sum_{t=1}^{N} r(t)$.

2. Use the Golden section search to locate the minimum of $\hat{D}(\theta) = |\hat{M}(\theta) - \hat{M}(\theta_0)|$ where $\hat{M}(\theta)$ is a numerical approximation of $M(\theta)$ based on $\hat{M}(\theta_i) = \frac{1}{N}\sum_{t=1}^{N} x_{\theta_i}(t)$ and $\{x_{\theta_i}(t) | t = 1,2,3,\cdots\}$ is the data sequence generated by the dynamical system $x(t) = f_\theta(\mathbf{x}(t-1))$ given in (3.1) with $\theta = \theta_i$.

3. According to Theorem 2, we know that $\hat{D}(\theta)$ is a consistent estimator of $D(\theta)$ and hence the unique minimum of $\hat{D}(\theta)$ is equivalent to that of $D(\theta)$.

3.2 Performance evaluation of the mean value method

Two popular chaotic systems, namely, the Tent map and the Chebyshev map [31] are used here to illustrate the effectiveness of the proposed method. The Tent map is defined by

$$T_\theta(x) = \theta - 1 - \theta |x| \tag{3.5}$$

where $x \in [-1, 1]$ and $\theta \in (1, 2]$, and the Chebyshev map is defined by

$$C_\theta(x) = \cos(\theta \cos^{-1}(x)) \tag{3.6}$$

where $x \in [-1, 1]$ and $\theta \in (1.3, 2]$.

The mean value functions of both maps are rather difficult to derive analytically. Using numerical techniques, we plot the mean value functions of both maps in Figures 3.1 and 3.2 respectively. The mean value function of the Tent map is not monotone over the entire parameter range but is monotonic increasing over the range $\theta \in [-1.1, -1.6]$. The mean value function value is over the range of about [0.04, 0.17]. On the other hand, the Chebyshev map has a monotone mean value function over the whole parameter range. Its mean value function is over a larger range of [-0.84, 0]. The proposed method can therefore be applied to these maps for parameters over the ranges with monotone mean value function.

Figures 3.3 and 3.4 depict the objective function $D(\theta)$ for the Tent map and Chebyshev map respectively. θ_0 in both cases are selected randomly over the parameter range with monotone mean value function as shown in Figures 3.1 and 3.2. Apparently, $D(\theta)$ in both Figures 3.3 and 3.4 are unimodal functions and hence the global minima for both functions can be obtained easily. Since we do not have the analytical form of the $M(\theta)$ for these maps, we have to use the approximation $\hat{M}(\theta)$. To understand the accuracy of the approximation, we plot the estimation variance of the mean value function of the Tent map versus the number of samples in Figure 3.5. It can be seen that the simulated performance is very close to the theoretical performance derived in Theorem 3. With the increasing sample numbers, the estimation variance decreases. Furthermore, the theoretical estimation variance is shown to be a function of sample numbers as well as the additive noise variance and hence we show the estimation variance in a 3-dimensional plot in Figure 3.6. In the figure, the estimation variance is affected by both the sample numbers and the variance of the AWGN noise. The simulated performance is quite consistent with the theoretical performance. Similar analysis is performed on the Chebyshev map, and the results are plotted in Figures 3.7 and 3.8. Again, the simulated estimation variances are very close to the theoretical performance given by Theorem 3.

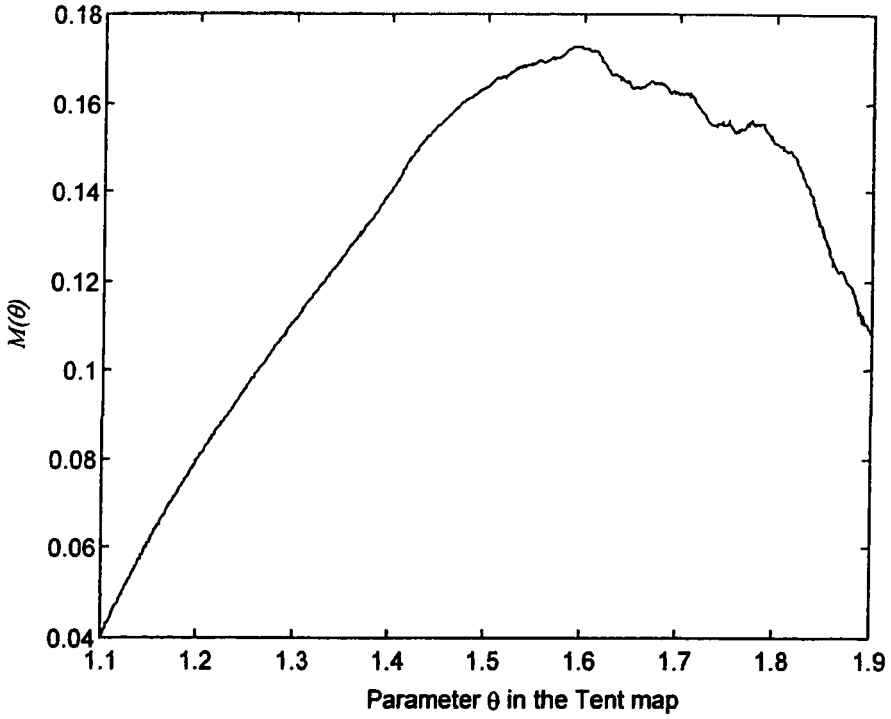

Figure 3.1. The mean value function $M(\theta)$ of the Tent map.

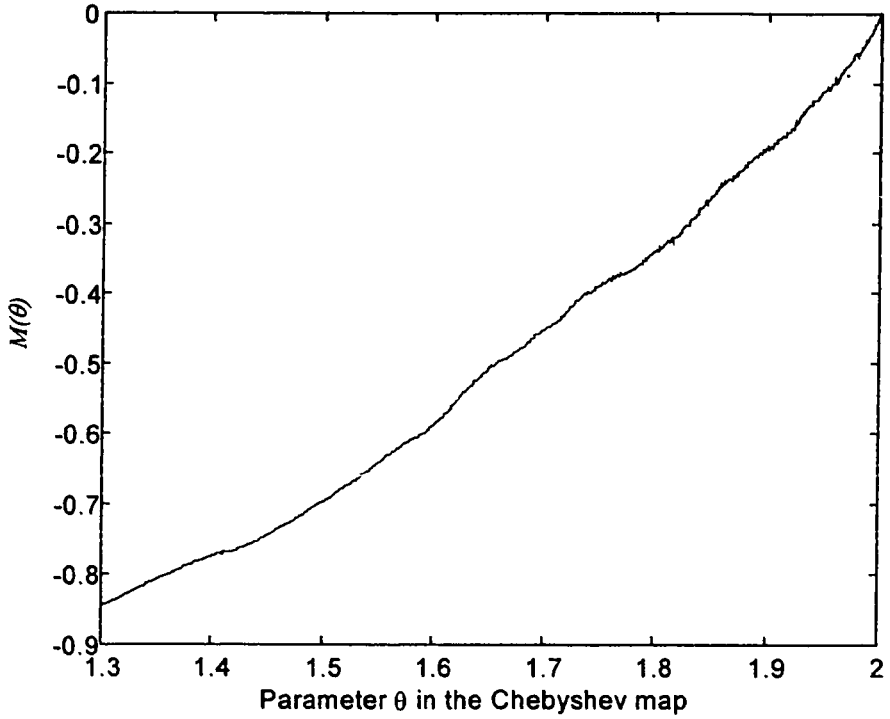

Figure 3.2. The mean value function $M(\theta)$ of the Chebyshev map.

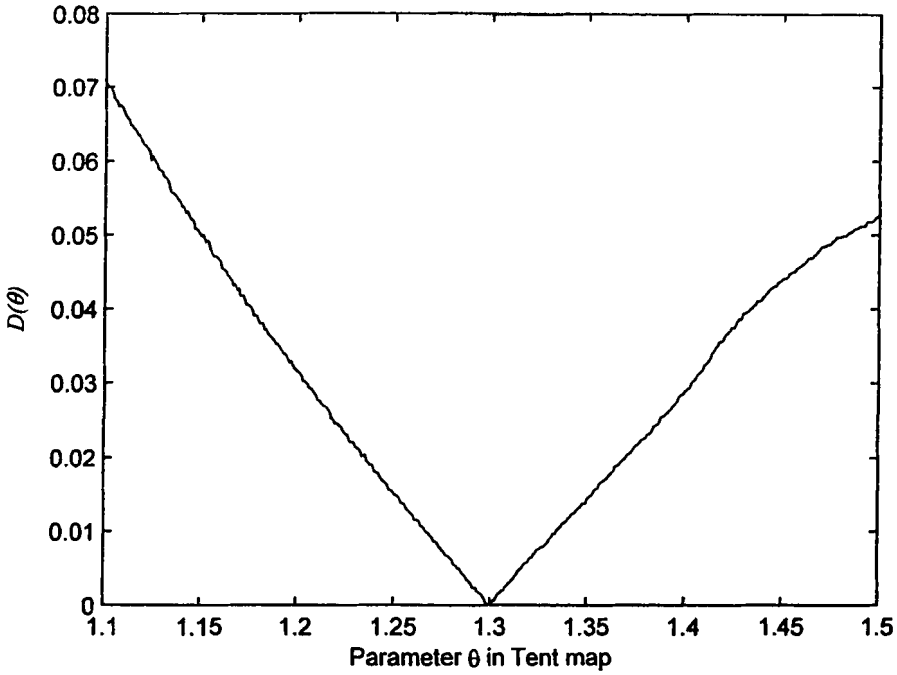

Figure 3.3. The unimodal optimization function $D(\theta)$ for the Tent map with θ_0=1.3.

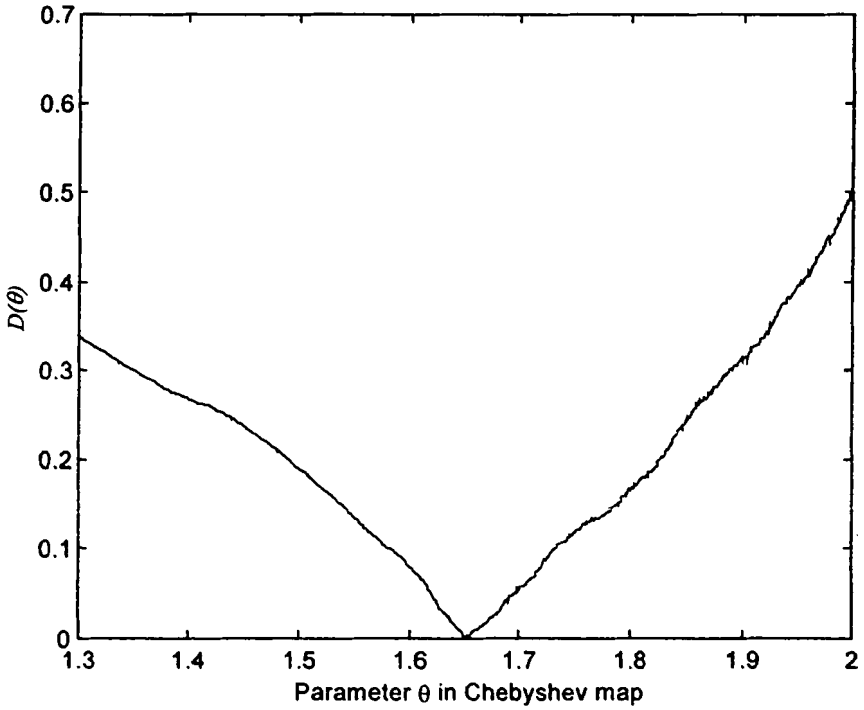

Figure 3.4. The unimodal optimization function $D(\theta)$ for the Chebyshev map with θ_0=1.65.

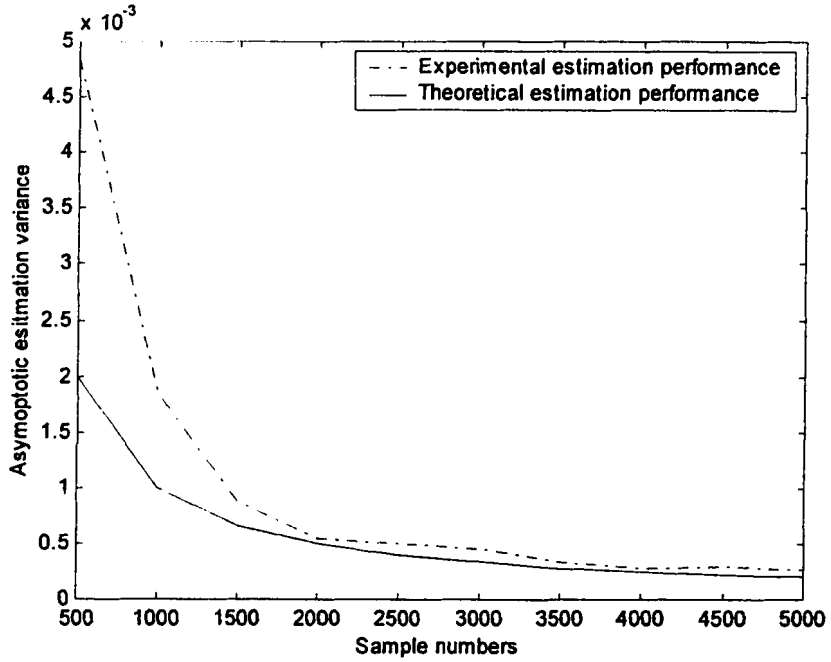

Figure 3.5. Asymptotic estimation performance of the Tent map with various sample numbers for estimation without measurement noise.

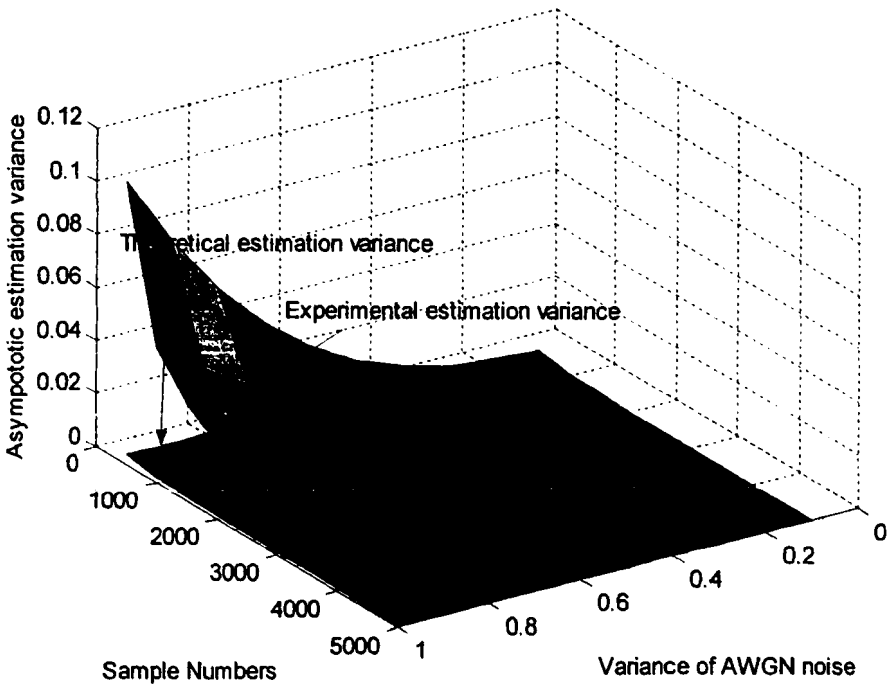

Figure 3.6. Asymptotic estimation performance of the Tent map versus the number of sample points and the variance of AWGN. The average power of the chaotic signal is assumed to be unity.

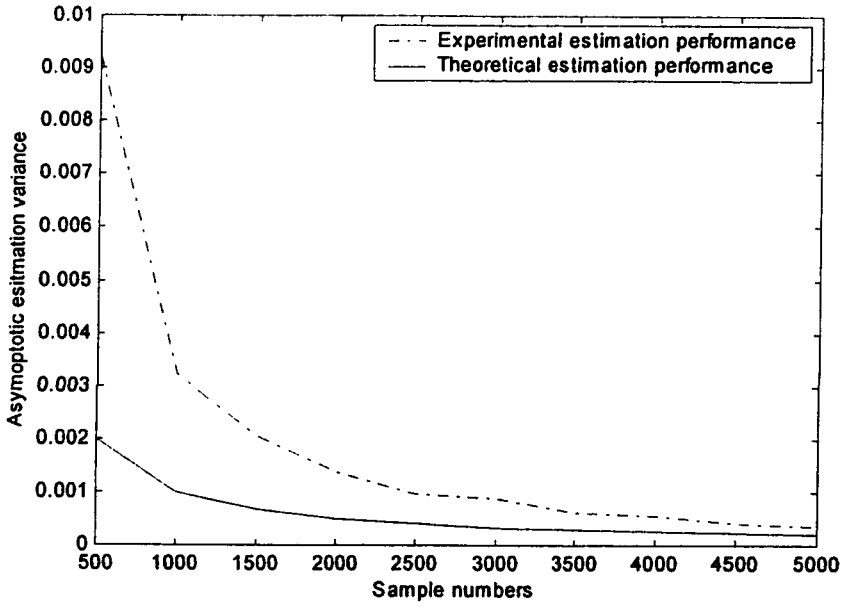

Figure 3.7. Asymptotic estimation performance of the Chebyshev map with various sample numbers for estimation without measurement noise.

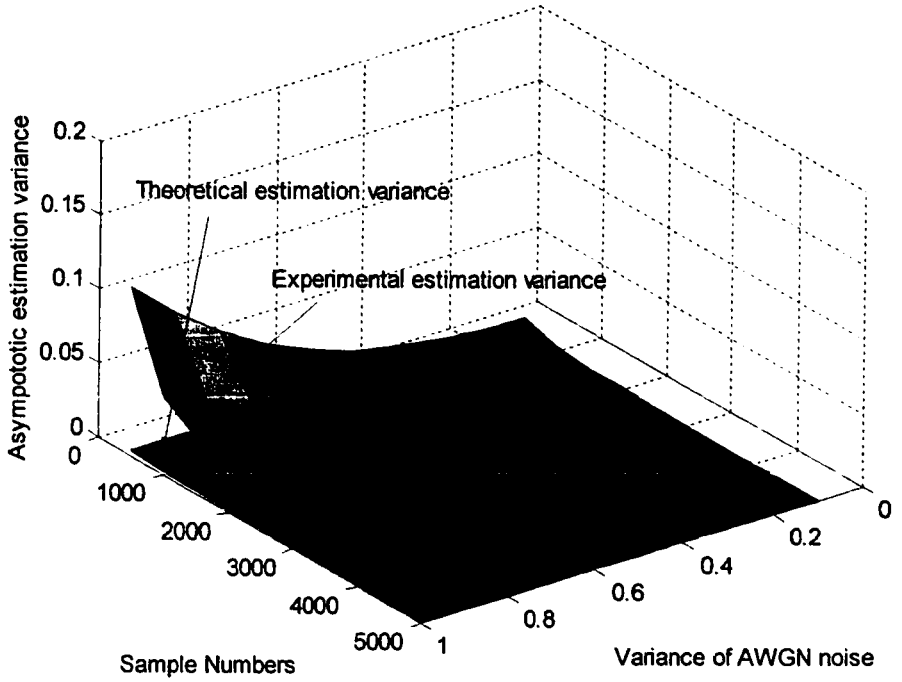

Figure 3.8. Asymptotic estimation performance of the Chebyshev map versus the number of sample points and the variance of AWGN. The average power of the chaotic signal is assumed to be unity.

Monte Carlo simulation is now carried out to evaluate the accuracy of the parameter estimates. The mean square error (MSE) in the parameter is evaluated versus various levels of SNR. The range of SNR considered in our study is from –20dB to 20 dB with an increment of 5dB. Each MSE value is computed by using an average of 100 trials. First, we assume that we have a very long signal sequence, that is, N is very large for the signal set $\{r(t) \mid t = 1,2,\cdots,N\}$. Since the proposed method relies on the ensemble average formula and as $N \to \infty$ the proposed method should show the ideal performance. We also implement two standard parameter estimation methods for comparison. The first one is the gradient search technique [40], which searches for an optimal estimate of θ along the direction of the gradient of error function. The derived iterative equation is given by (2.15) where f_θ can be either T_θ or C_θ. The second standard technique is the nonlinear least square method based on the Gauss Newton method, and our implementation of the second method is based on the MATLAB function "NLINFIT". For the details of the Gauss Newton method, the readers are referred to [41] which shows the iterative equations for this nonlinear least squares method.

The MSE curves of these three methods for the Tent map are depicted in Figure 3.9. The nonlinear LS and gradient search methods have fairly close performances. For higher SNR, say about 20dB, all three estimation methods have fairly close MSE performances. The mean value method is only about 5dB better than the two standard techniques. However, when the noise level increases, the improvement of the mean value method becomes more significant. From Figure 3.9, if N is sufficiently large and hence the noise mean is almost exactly equal to zero, the estimation accuracy of the proposed method is almost independent of the measurement noise. The MSE value of the mean value estimation method remains at about –55dB for all SNR between –20 to 20dB. The difference in MSE between the proposed method and the two standard techniques at $SNR = -20\ dB$ is about 60dB according to Figure 3.9.

The MSE curves for the Chebyshev map are plotted in Figure 3.10. Because of the high nonlinearity in the Cheybeshev map, both standard methods are not quite effective even when the SNR is high. However, the proposed mean value estimation method is apparently is almost unaffected by such nonlinearity of the chaotic map. It can still improve the estimation accuracy significantly. In this experiment, when the signal

sequence is very long, the estimated mean values of the signal and noise processes are almost equal to their exact theoretical values. The mean value estimation method can estimate the parameter of the Cheybeshev accurately (around –55dB) even when the SNR is as low as –20dB. Compared to the two standard methods, the improvement is again about 60dB.

In the second experiment we reduce the length of the signal sequence N to 2000. The estimation results for the Tent map and the Chebyshev map are plotted in Figures 3.11 and 3.12 respectively. The two adaptive filter methods do not seem to be affected by this reduction of data sequence length, and their MSE curves remain almost exactly the same as those in the first experiment. However, for the mean value method, due to the use of finite sequence, the ensemble average will introduce some errors in the mean value estimation for both the chaotic signal and the AWGN signal. The performance of the proposed mean value method is therefore degraded as discussed above. When SNR is low, a small error in the mean value estimation will produce a relatively large impact on the parameter estimate. Compared with that of infinite sequence, the mean value method degrades about 40dB for both maps at SNR = -20dB. However, compared with the two standard methods, the mean value method still has about 20dB improvement. For the Chebyshev map, this 20dB improvement is almost like a constant over the entire range of SNR values.

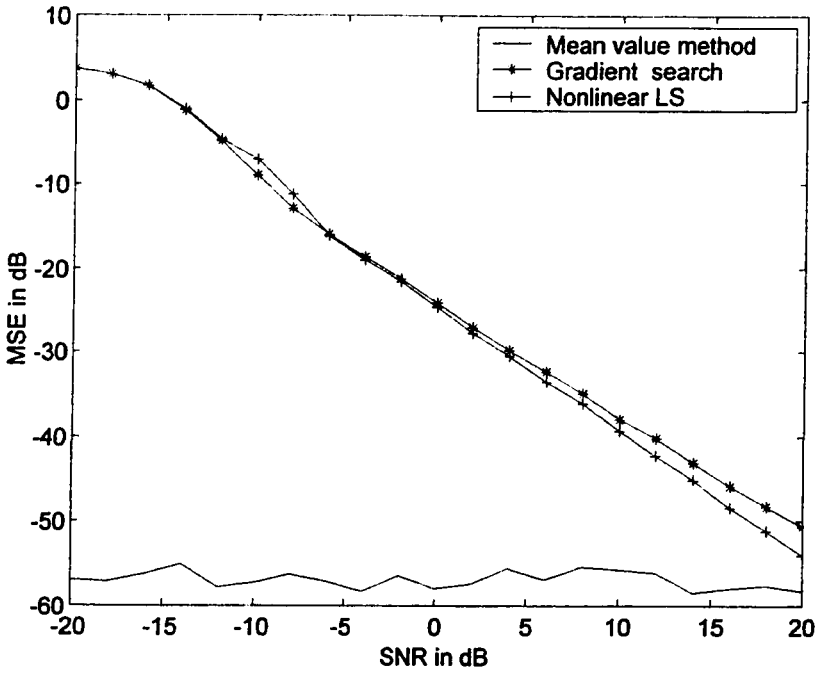

Figure 3.9. Performance evaluations of various parameter estimation methods for the Tent map under AWGN with exact zero mean. The parameter θ_0 is selected randomly on [1.1, 1.5].

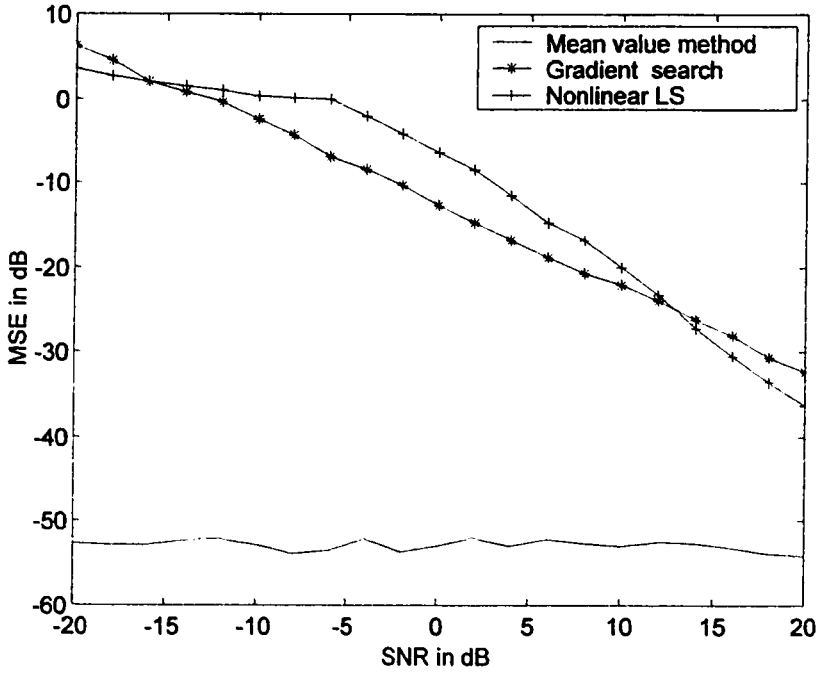

Figure 3.10. Performance evaluations of various parameter estimation methods for the Chebyshev map under AWGN with exact zero mean. The parameter θ_0 is selected randomly on [1.3, 2].

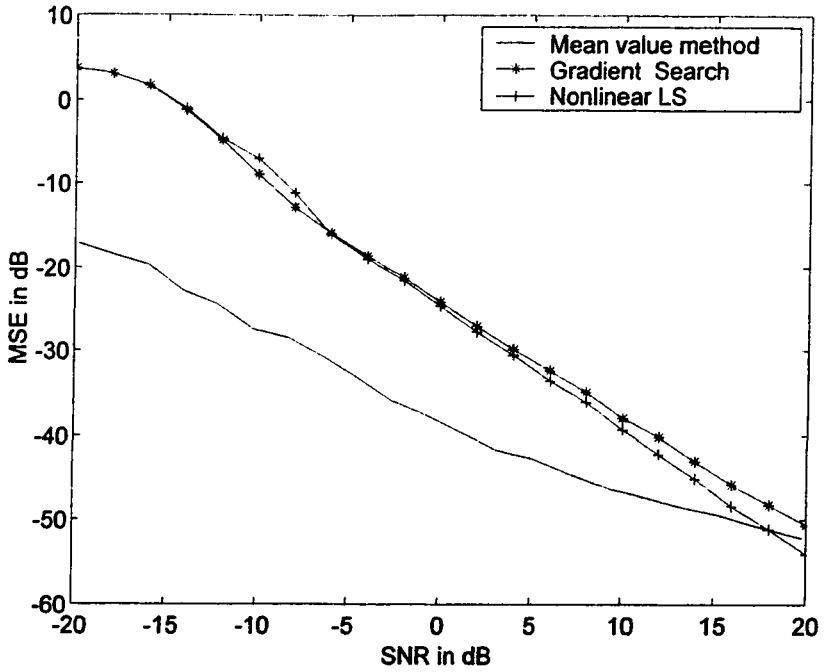

Figure 3.11. Performance evaluations of various parameter estimation methods for the Tent map under AWGN with non-exact zero mean. The parameter θ_0 is selected randomly on [1.1, 1.5].

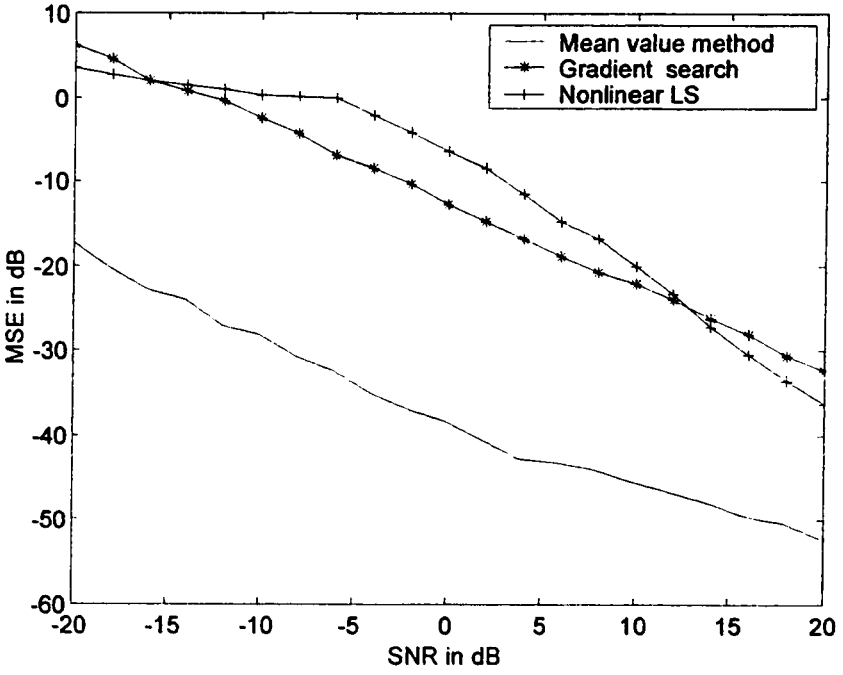

Figure 3.12. Performance evaluations of various parameter estimation methods for the Chebyshev map under AWGN with non-exact zero mean. The parameter θ_0 is selected randomly on [1.3, 2].

3.3 Applications to SS digital communication system

The chaotic SS communication system considered here is based on the CPM method. It is called ergodic CPM (ECPM) system in our study. Assume that *s(t)* is the message signal, the chaotic modulation method uses a chaotic system

$$x(t) = f_\theta(x(t-1),\cdots,x(t-d)) \tag{3.7}$$

to modulate *s(t)* by setting $\theta = s(t)$ or in general $\theta = g(s(t))$, i.e. a function of *s(t)*. Since one-dimensional system is used in our communication system, $d = 1$. By keeping θ in the chaotic regime, the output signal *x(t)* is therefore chaotic and hence has a wide bandwidth for spread spectrum transmission.

For digital communications, the message signal *s(t)* takes on only two values within each bit duration, that is, "0" or "1" at $t \in [0, T_b]$. Therefore, in the modulation process, only two parameter values are needed to represent the message signal. That is,

$$\theta = \begin{cases} \theta_0 & if \quad s(t) = 0 \\ \theta_1 & if \quad s(t) = 1 \end{cases}. \tag{3.8}$$

The demodulation process therefore does not require estimation of a wide range of parameters but only two values θ_0 and θ_1. To apply the mean value estimation to the demodulation process, an obvious necessary condition is that θ_0 and θ_1 should not have the same mean value, that is, $M(\theta_0) \neq M(\theta_1)$. Without loss of generality, we can choose θ_0 and θ_1 such that $M(\theta_1) > M(\theta_0)$. The mean value estimator demodulates the received noisy signal $r(t) = x(t) + n(t)$ by determining whether the parameter used to generate *x(t)* is θ_0 or θ_1. The basic idea of the proposed ECPM digital communication system is depicted in Figure 3.13.

Since the Chebyshev map is demonstrated to have a good performance for this ergodic approach in the previous section, it is employed in our ECPM communication system. The detailed block diagram of this new chaotic communication scheme is illustrated in Figure 3.14. The binary information data *s(t)* ("0" or "1") with frequency f_b is spread and modulated by the chaotic signal *x(t)*. The chaotic signal *x(t)* is generated by the Chebyshev map in (19) with only two possible parameter values: $\theta_0 = 1.3$ or $\theta_1 = 2$, that is,

$$x(t) = C_{\theta_i}(x(t-1)), \quad i = 0,1 \tag{3.9}$$

where $t \in [0, T_b]$.

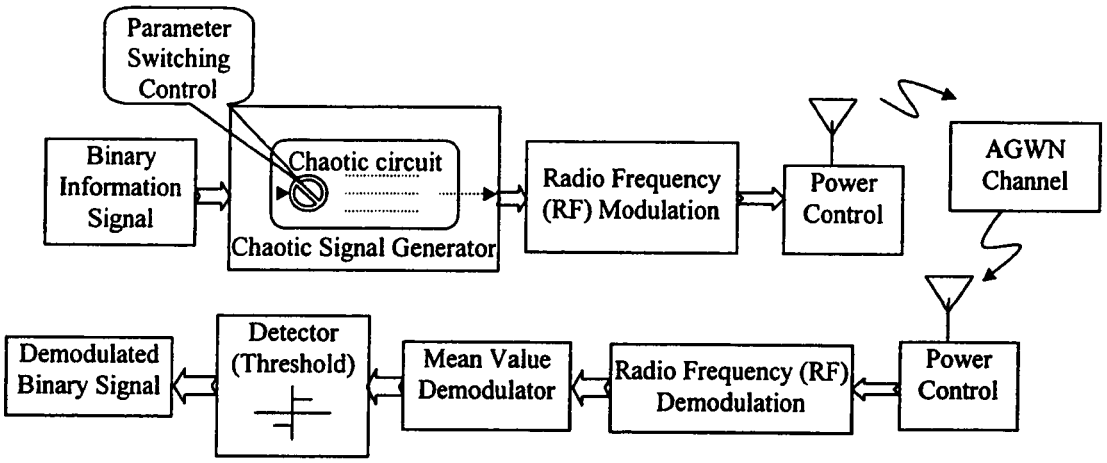

Figure 3.13. Block diagram of ergodic chaotic parameter modulation (ECPM) communication system.

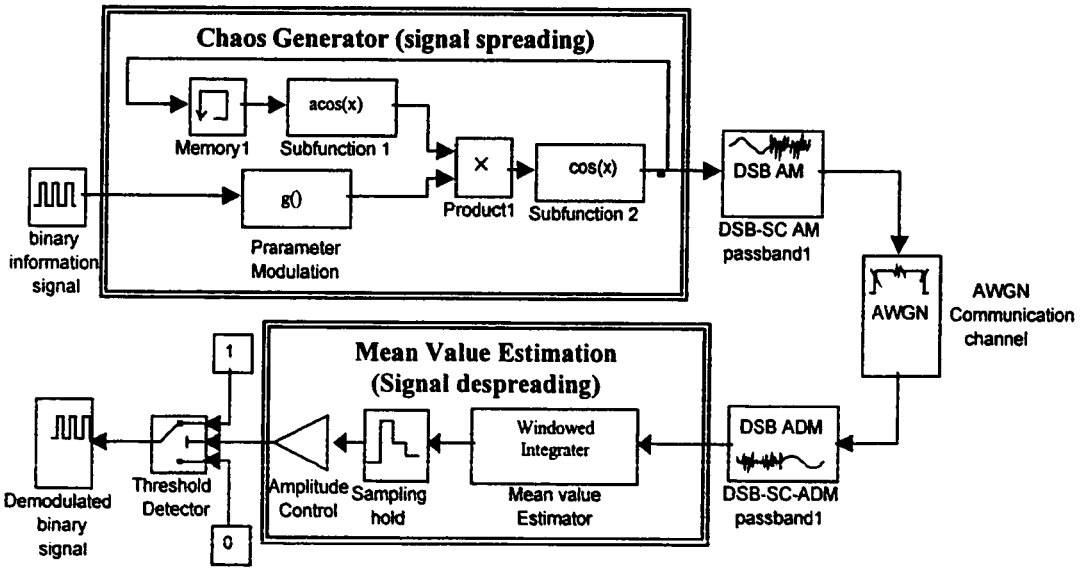

Figure 3.14. Detailed simulation model of the proposed ergodic chaotic parameter modulation (ECPM) system based on the Chebyshev map for SS digital communications.

If the step size between two adjacent states of the Chebyshev maps is T_x, then the ratio of the chaos generation rate f_x: $f_x = 1/T_x$, to the data rate f_b can be considered as the processing gain G of this chaotic SS system. That is,

$$G = \frac{T_b}{T_x} = \frac{f_x}{f_b}. \tag{3.10}$$

In other words, each data bit is represented by G samples of the chaotic signal generated by the Chebyshev map.

The chaotic modulated wideband signal is then modulated to the radio frequency (RF) for transmission. The amplitude modulation (AM) is employed in our simulation model. At the receiver end, a demodulator is applied to move the received RF carrier back to the baseband. After the RF demodulation, the noise corrupted received signal $r(t) = x(t) + n(t)$ is passed to the chaotic demodulator. $n(t)$ is the channel noise and is usually assumed to be white Gaussianly distributed.

In the proposed demodulator, the mean value of $r(t)$ is first estimated using the ensemble average. The output of the mean value estimator is sampled with frequency f_b and $f_b = 1/T_b$. The sampled output of the k^{th} bit transmitted signal can then be expressed as:

$$\begin{aligned} m_k &= \frac{1}{T_b}\int_{kT_b}^{(k+1)T_b} r(t)dt \\ &= \frac{1}{T_b}\int_{kT_b}^{(k+1)T_b} x(t)dt + \frac{1}{T_b}\int_{kT_b}^{(k+1)T_b} n(t)dt \\ &= \hat{M}(\theta_i). \end{aligned} \tag{3.11}$$

Since x(t) is generated by (3.6) and the expectation of an AWGN process is zero, if the T_b is large enough, the estimator $\hat{M}(\theta_i)$ approaches $M(\theta_i)$.

$$m_k \approx M(\theta_i). \tag{3.12}$$

To decode the message signal $s(t)$ in the k^{th} bit, we need to determine θ_i from m_k. Based on the fact that $M(\theta)$ is monotone for the Cheybshev map, θ_i can be estimated by $\theta_i \approx M^{-1}(m_k)$. But since θ_i only takes on two values for binary digital communications, the demodulation process can in fact be further simplified to a binary decision process. That is,

$$\hat{s}(t) = \begin{cases} 1, & if \quad m_k \text{ is closer to } M(\theta_1) \\ 0, & if \quad m_k \text{ is closer to } M(\theta_0) \end{cases}. \tag{3.13}$$

More precisely, a threshold on the mean value μ_M is set for decision-making. That is,

$$\hat{s}(t)=\begin{cases}1, & if \quad m_k > \mu_M \\ 0, & if \quad m_k \le \mu_M\end{cases}. \tag{3.14}$$

In this study, we choose the threshold μ_M to be the midpoint between $M(\theta_0)$ and $M(\theta_1)$, that is, $\mu_M = \dfrac{M(\theta_1)+M(\theta_0)}{2}$.

It should be noted that according to Theorem 3, the asymptotic variance of the estimated mean value function is equal to $\dfrac{\delta_x^2+\delta_n^2}{N}$, where δ_x^2 is the average power of the chaotic signal, δ_n^2 is the average power of the AWGN, and N is the number of samples which is equal to the processing gain in this SS application, i.e. $N = G$. Since G cannot really approach infinity in practice, unless we can estimate the noise mean over the bit duration and subtract it from the signal, it is favorable to maximize the distance between $M(\theta_0)$ and $M(\theta_1)$ to minimize the noise effect. To do that, the chaotic carrier $x(t)$ can be normalized at the transmitter side by strictly fixing its mean value within each bit duration as constants. That is,

$$x'(t) = x(t) - \int_0^{T_b} x(t)dt + M(\theta_i). \tag{3.15}$$

What's more, in order to set the threshold μ_M of the detector at the receiver to be zero, which will not be affected by the transmitted SNR level any more, we can further normalize the chaotic signal by minus μ_M from the chaotic signal. That is,

$$x'(t) = x'(t) - \mu_M. \tag{3.16}$$

Thus, at the output of the demodulator, we can simply employ a zero threshold detector, $\mu_M = 0$, to determine which data symbol is transmitted. That is,

$$\hat{s}(t)=\begin{cases}1, & if \quad m_k > 0 \\ 0, & if \quad m_k \le 0\end{cases}, \tag{3.17}$$

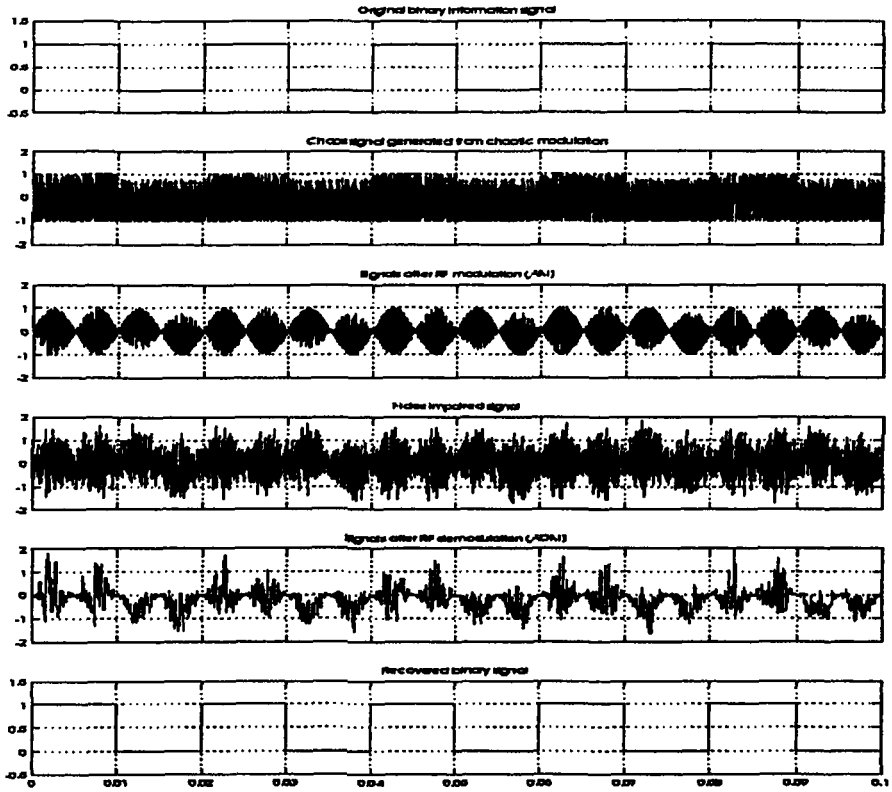

Figure 3.15. Signal waveforms in various stages of the ECPM communication system.

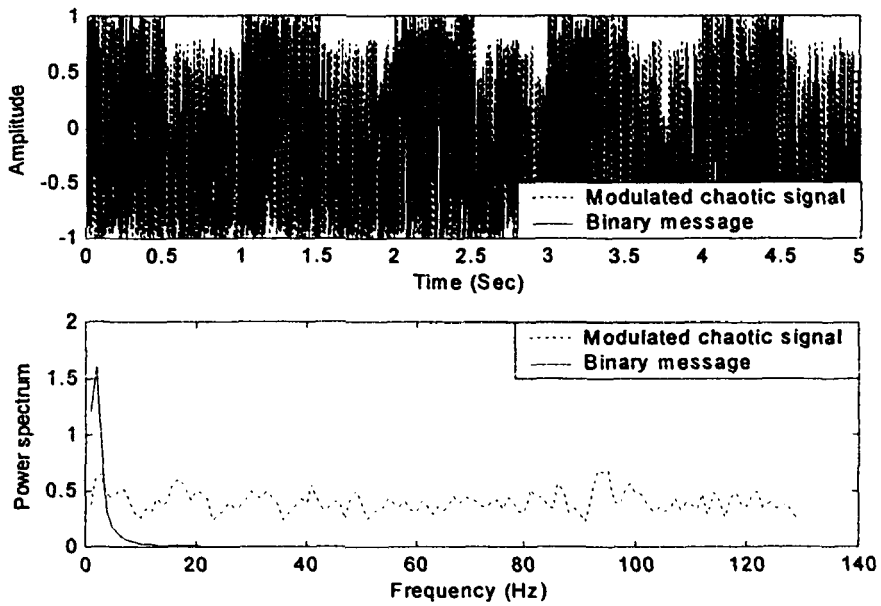

Figure 3.16. The time waveform and power spectrum density of the original binary message and modulated chaotic signal.

Figure 3.15 shows the signal waveforms at various stages of the proposed ECPM communication system. The original messages, chaotic modulated signals and RF modulated signals are shown in the first three diagrams in Figure 3.15. The received and final demodulated signals are displayed in the last two diagrams in Figure 3.15. We also plot the time waveforms of the signals and their corresponding power spectra in Figure 3.16. As we can see, the chaotic modulated signal indeed has a random appearance and a relatively wide spectrum for SS communications.

It should be pointed out that there are many advantages of the proposed ECPM communication system. First, it is computationally very simple, and hence the cost for hardware implementation is very low. In fact, the proposed demodulator is even simpler than the conventional correlator for SS communications. It only consists of several additions and one multiplication for discrete signals and an integrator for analog implementation. Second, it does not require the complicated synchronization procedure. As shown in [9], comparing to other chaos communication schemes, parameter modulation is the only one that is totally unaffected by synchronization errors. Third, the proposed system uses a non-coherent demodulator which makes the implementation even simpler.

But to claim whether the ECPM scheme is useful for communications, its noise performance based on bit error rate (BER) must be evaluated. To have a better understanding of the effectiveness of the proposed new scheme, we also implement the AF-CPM system by using the gradient search method as demodulator.

Let E_b and N_0 denote the energy per bit and the power spectral density of the AWGN respectively. We compute the BER versus the E_bNR to evaluate the performance of these chaos modulation communication schemes where E_bNR is the ratio of E_b to N_0. For all these two CPM systems, the Chebyshev map is employed as the chaos generator. They all employ the simple amplitude modulation (AM) as RF modulation. The RF central frequency f_c is set as 10 MHz. In our study, we set the chaotic generation rate f_x, or the controlling frequency of the chaotic system is equal to the RF frequency. The processing gain of the system is of 1000.

Similar to the estimation study in the previous section, the first experiment considers the situation where the mean value of the AWGN is extremely close to zero. In

fact, we can also assume that the noise mean can be estimated accurately. The estimated noise mean value is therefore completely subtracted from the received signal. In this ideal situation for ergodic theory, we plot the BER of ECPM and AF-CPM in Figure 3.17. A very interesting observation is that the proposed ECPM system can achieve a perfect communication performance. That is, it can demodulate the transmitted binary signal without any error regardless of the noise power measured in the channel. This interesting observation really shows the potential of chaos communications. Compared to AF-CPM, the BER of ECPM is significantly better than the other.

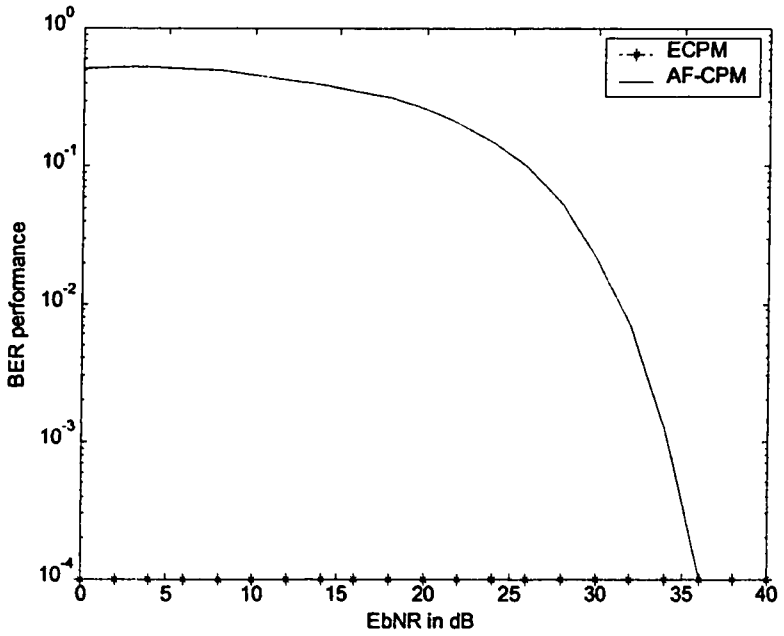

Figure 3.17. Comparison of the BER performance of various CPM systems in AWGN channel with exact zero mean noise.

In the second experiment, the noise mean value over different bit duration will not equal to zero exactly. We also assume that it is difficult to estimate the noise mean accurately and hence do not perform any cancellation or modification on the simulated noise mean. Because of the short sequence length, the bias in the noise mean will introduce some error in the demodulation process of the ECPM scheme. The BER performances of ECPM and AF-CPM systems in AWGN are shown in Figure 3.18. Apparently, the proposed ECPM communication system still has better performance than the AF-CPM system.

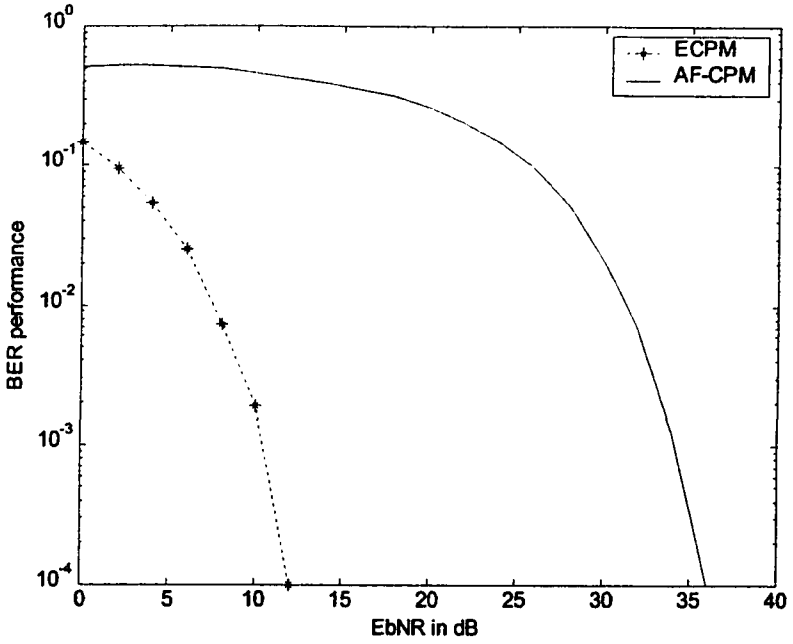

Figure 3.18. Comparison of the BER performance of various CPM systems in AWGN channel with the noise mean is not exactly zero.

CHAPTER 4

COMPARATIVE EVALUATION OF CHAOS BASED SS COMMUNICATION SYSTEMS WITH VARIOUS CONDITIONS

To have a better understanding of the strong and weak points of the proposed ECPM communication system, it is necessary to perform a comprehensive evaluation of the ECPM scheme with other major chaos based schemes described in Chapter 2. Although many active ongoing researches have been carrying out for the chaos communication schemes, not much of them have been done on evaluating and comparing their performances [8,9]. It is our objective here to conduct such a comparative performance evaluation of all these chaos based SS communication schemes, including the ECPM, on a common digital communication platform as shown in Figure 1.3. Several important factors are used in the evaluation, including the noise performance, robustness to synchronization error, capacity for high data rate transmission and immunity for the multi-path effect. These factors are chosen since they are most fundamental elements for a practical digital SS communication system to-date.

4.1 Chaotic SS digital communication platform

A computer simulation model is developed here as a general platform to evaluate the performance of all chaotic digital communication schemes, including CSS, CC, CCSK, NCSK, FM-DCSK, CM, AF-CPM and ECPM. This communication platform is implemented using MATLAB and is based on the Monte-Carlo simulation model [43]. Since all these chaotic communication schemes are implemented on a common ground, this communication platform is suitable to carry out comparative evaluation of these schemes under different communication conditions.

The one dimensional Chebyshev map $x(t) = \cos[\theta \cdot \cos^{-1}(x(t-1))]$ as in (3.6) is employed here as the chaotic state function. The controlling frequency f_x of the chaotic system determines the chaotic signal generation rate or the step size T_x ($= 1/f_x$) between two adjacent states. In our study, f_x is assumed to be the same as the transmitted

bandwidth B_w, and is fixed as $B_w = f_x = 10\,MHz$ throughout this simulation, which can be seen as the condition of coaxial cable channels. The processing gain G of the systems is considered as $G = f_x / f_b$ in (3.10). The binary information data *s(t)* ("0" or "1" within each bit duration) with data rate f_b is spread and modulated by the chaotic signal *x(t)*, and $T_b = 1/f_b$ is the bit duration. For the CSS, CC, FM-DCSK and CM schemes, *x(t)* is generated with Chebyshev map of $\theta = 2$. For the other chaotic schemes including CCSK, NCSK, AF-CPM and ECPM, two parameter values are required and we set $\theta_0 = 1.3$ and $\theta_1 = 2$ to generate chaotic signal waveforms for their applications. It should be noted that the CSK scheme is supposed to have two different state functions f_0 and f_1 for signal transmission. But to reduce the ambiguity of the comparison, we avoid using a different state function that is used in CSK alone. Instead, we use θ_0 and θ_1 in the Chebyshev map to generate two signal waveforms for CSK application since these signal waveforms are also uncorrelated and have different bit energies in the same bit duration. We plot the phase space portrait of Chebyshev map in Figure 4.1 for $\theta = 2$.

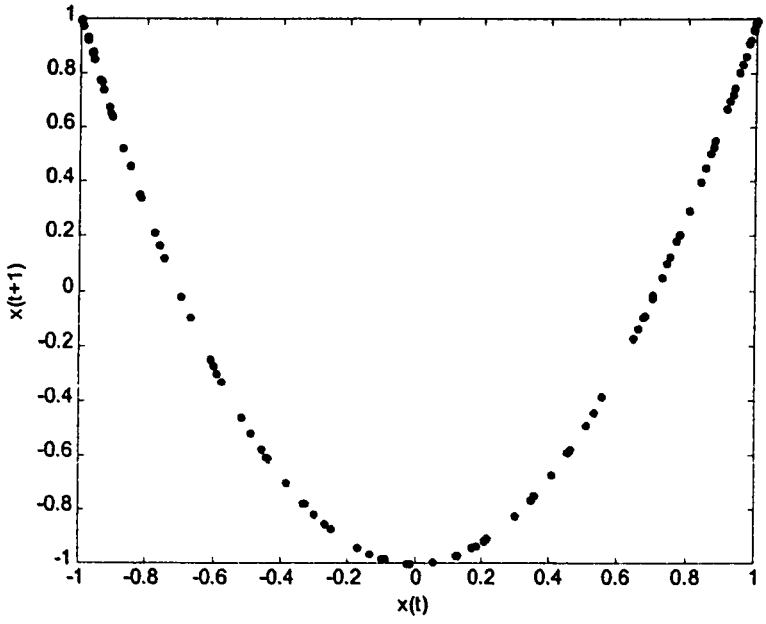

Figure 4.1. Phase space portrait of the Chebyshev map with $\theta = 2$.

To characterize the communication performance, the bit error rate (BER) as a function of the ratio of the signal energy per bit E_b to the noise spectral density N_0 (E_bNR), is used here as the measure criterion. In terms of RF transmission, the signal to

noise ratio (SNR) can be used instead of E_bNR. As a matter of fact, E_bNR and SNR are basically related. Noting that the total spread wide bandwidth of the RF channel is B_w and the bit duration of the binary data is T_b, the SNR at the input of the demodulator can be described as a function of E_bNR as follows:

$$SNR = \frac{P_s}{P_n} = \frac{E_b}{N_0}\frac{1}{B_w T_b} = \frac{E_b}{N_0 G}. \tag{4.1}$$

In many applications, the SNR at the RF domain may be as low as 0dB.

In a practical chaos based SS communication system, the binary information signal to be transmitted is first modulated by the chaos based modulation schemes; that is, the information signal is spread or mapped to a broadband noise-like signal. The broadband signal is then converted up to the radio frequency (RF) by some RF modulation. For FM-DCSK, apparently the frequency modulation is applied. For CSS and CC, the binary phase shift keying (BPSK) technique is used for RF modulation as in the standard DSSS system. For the other schemes, the basic amplitude modulation is employed. After RF demodulation, the signal is fed into the chaos based demodulators. For the non-coherent demodulation schemes such as NCSK, FM-DCSK, AF-CPM, ECPM and CM, the demodulator will process the demodulation on the received noisy signal directly. But for those coherent demodulation schemes like CSS, CC and CCSK, a synchronized reference signal has to be supplied to perform the correlation with the received signal. Note that the low-pass equivalent model is used for simulation. It gives directly the relationship between the transmitted signals and channel noise. The carrier frequency has been removed completely and only low-pass signals appear in the simulation model so simulation time is minimized.

4.2 Noise performance in an AWGN channel

One of the most important performance measures of a communication system is its performance in a noisy channel. And the most popular model is the additive white Gaussian noise (AWGN) channel. The standard theoretical construction of this kind of front-end noise can be fairly well approximated in simulation over a bandwidth that is at least as large as that of the receiving system [1,43]. Further more, the generated

independent noise samples vary at the same rate with the frequency bandwidth. The basic model of the received signal is usually expressed by

$$r(t) = x'(t) + n(t), \tag{4.2}$$

where $x'(t)$ is the modulated signal and $n(t)$ is an AWGN process with uniform power spectral density $\phi_{nn}(f) = \delta_n^2 = N_0$ W/Hz. The performance of a communication system is evaluated by the bit error rate (BER), which counts the average number of bit errors for specified channel conditions. A digital communication system is typically expected to perform with a BER of less than 10^{-3} [1,13].

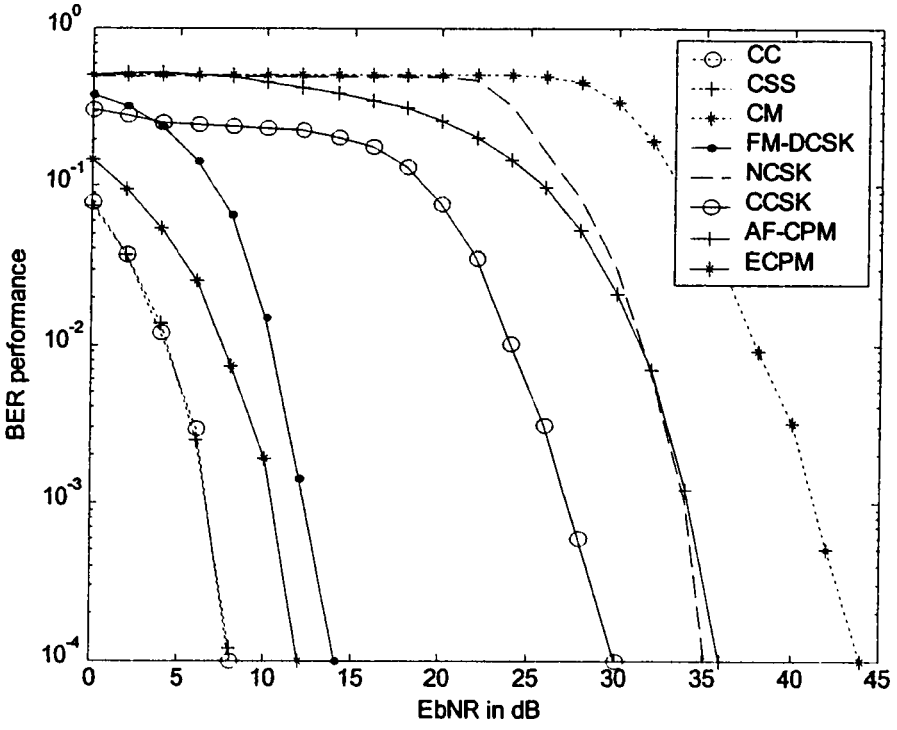

Figure 4.2. Noise performance of the different chaos based schemes in an AWGN channel.

Figure 4.2 shows the BER of all the chaos based communication schemes considered here in an AWGN channel. The simulation is based on a data rate of $f_b = 50\,kbps$, the bit duration is $T_b = 20\,\mu s$. This is approximately a practical low speed for the data transmission, i.e. in the telephone line modem. Since the system has a fixed chip rate of $10\,MHz$, for this data speed, the corresponding processing gain G is then

equal to 200. The required SNR at the demodulator input can be computed from the given E_bNR based on (4.1).

Note that the noise performances of CSS and CC are almost identical and their performances are also very close to that of the conventional DSSS system with the coherent BPSK modulation. The E_bNR value is about 7 dB at the BER level of 10^{-3}. The result should not be surprising since these two schemes are basically the same as the conventional DSSS system. The only difference is that the conventional PN sequence is replaced by a chaotic signal. Since the expectation of the chaotic signal generated from (20) with θ =2 is zero, the chaotic spreading sequence is converted from the chaotic signal $x(t)$ by modifying (2.1) to be given as

$$b(k) = g(x(t))_{t=kT_s}. \tag{4.3}$$

The autocorrelation performances of the chaotic spreading sequence and the chaotic carrier are plotted in Figure 4.3 for illustration. The advantages of CSS and CC over the conventional DSSS system are that the spread sequence or carrier can be produced easily and can be applied without the periodic constraint.

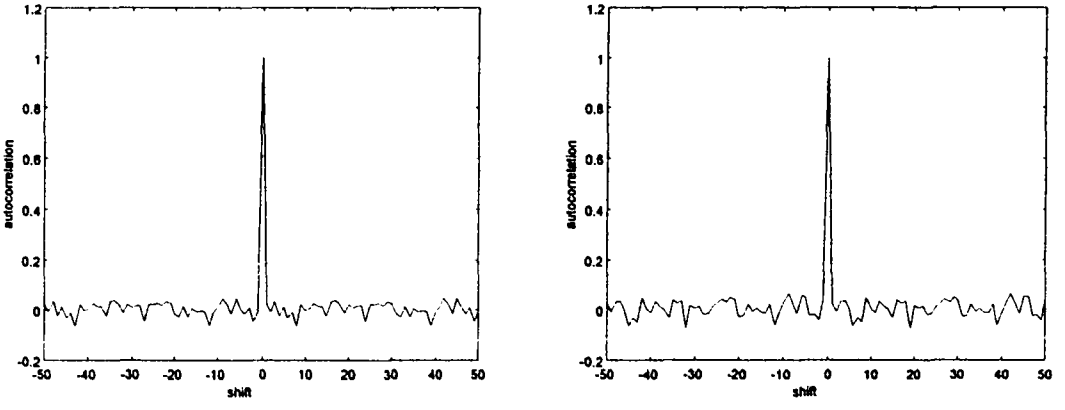

(a) (b)

Figure 4.3. Autocorrelation function of (a) the spreading sequence for the CSS approach and (b) the chaotic carrier for the CC method.

Unlike CSS and CC, the other chaos based communication systems have fairly different performances. According to Figure 4.2, the performance of ECPM [44] and FM-DCSK [45,46] are relatively close to that of the BPSK modulation. For BER = 10^{-3}, the E_bNR level of the FM-DCSK is about 13 dB, and the ECPM is about 2dB better than the FM-DCSK. For the ECPM scheme, the mean values of the chaotic signal generated from

(20) with $\theta_0 = 1.3$ and $\theta_1 = 2$ are equal to –0.9 and 0 individually. Thus the threshold of the detector in (3.14) is equal to –0.45. As a matter of fact, it is better to apply a zero-value threshold at the detector since it is not affected by the SNR level. We therefore normalize the chaotic signal by simply shifting it by a constant value –0.45 to achieve the threshold of zero at the receiver, as in (3.16).

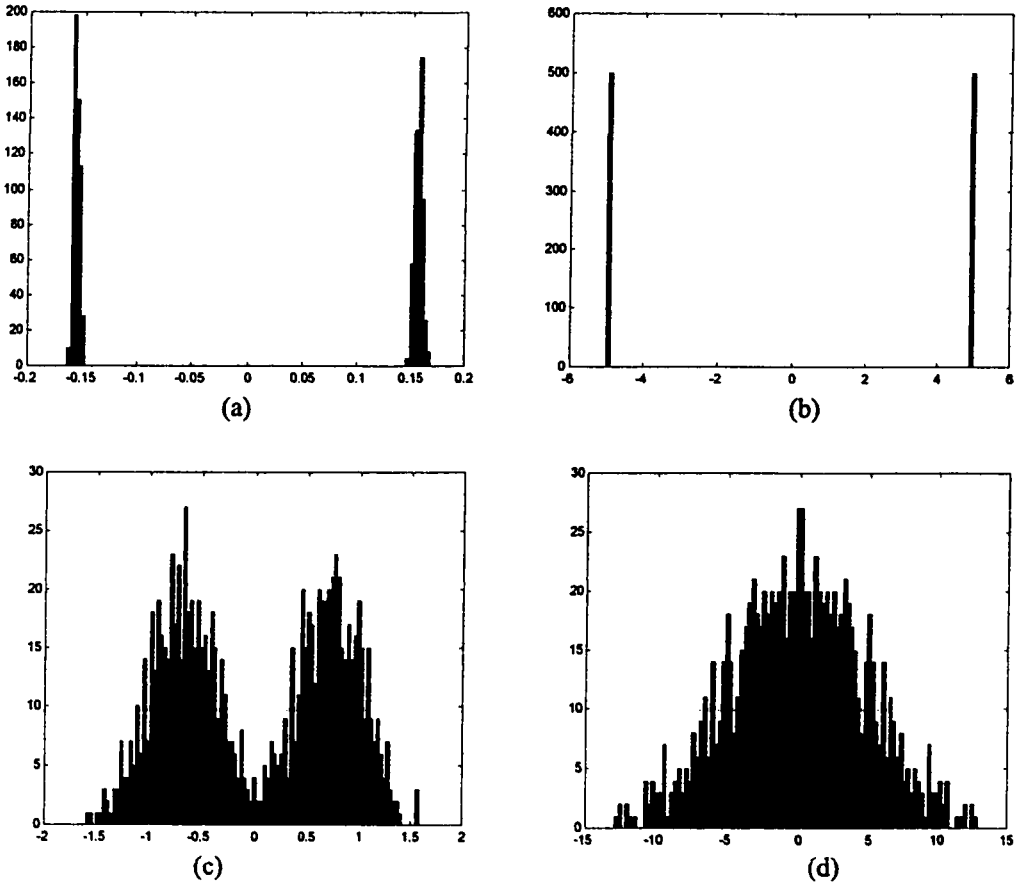

Figure 4.4. The histogram plots of the output signals of the demodulator of (a) ECPM and (b) FM-DCSK in a noise free environment, and (c) ECPM and (d) FM-DCSK in the noise environment of $E_b NR = 10\ dB$.

The histograms of the outputs of the demodulators of both ECPM and FM-DCSK for transmitting different digital symbols are plotted in Figure 4.4. In Figure 4.4 (a) and (b), the observed outputs for ECPM and FM-DCSK are plotted under the noise free condition, and in Figure 4.4 (c) and (d) the outputs are observed when the transmitted signal is corrupted by the channel noise with E_bNR = 10 dB. When the histograms for the two digital symbols overlap, detection error will be introduced in the demodulation process. Comparing Figure 4.4 (c) with 4.4 (d), the overlapping area for ECPM is

apparently smaller than that for FM-DCSK. Thus, the BER performance of the FM-DCSK is worse than that of the ECPM.

The performances of CCSK, NCSK, CM and AF-CPM are quite poor. Their E_bNR values are above 25 dB for a BER value of 10^{-3}. In the CCSK and CM implementation, the one way coupling chaotic synchronization system corresponding to the Chebyshev map is employed as the demodulator. That is,

$$\begin{cases} g_n = \cos[\theta \cdot \cos^{-1}(r(t-1))] - \cos[\theta \cdot \cos^{-1}(x_r(t-1))] - p \cdot [r(t-1) - x_r(t-1)] \\ x_r(t) = \cos[\theta \cdot \cos^{-1}(x_r(t-1))] + \varepsilon \cdot g_n \end{cases} \tag{4.4}$$

where p = 0.8, ε = 1, $x_r(t)$ is the reconstructed chaotic signal. Under the noise free condition, this approach can achieve perfect synchronization after a period of tracking as illustrated in Figure 4.5. When the signal is corrupted by measurement noise, there will be some synchronization errors. It is shown in [20,21] that even a small amount of noise will cause the systems to be desynchronised. Therefore, the performance of the signal recovery is very poor in a noisy environment [47]. Furthermore, for the CM implementation, the masked information level A has to be set as a very small value (= 0.1 in this study) in order to keep the modulated signal within the synchronization regime. This restriction puts a limit on the performance of CM, and its E_bNR is about 40 dB to achieve a BER of 10^{-3}. For the AF-CPM system, it has been reported that this approach has a poor performance when the SNR is low [22]. For the NCSK scheme, its performance is also reported to be poor in [8] since the output of the demodulator is most likely to be corrupted by the channel noise based on its demodulation rule.

Additionally, it should be noted that the performances of the CM, AF-CPM and NCSK are dependent on other system parameters except of SNR level. By selecting different chaotic systems, synchronization schemes, adaptive filtering algorithms or bifurcating parameters, their performances might appear differently.

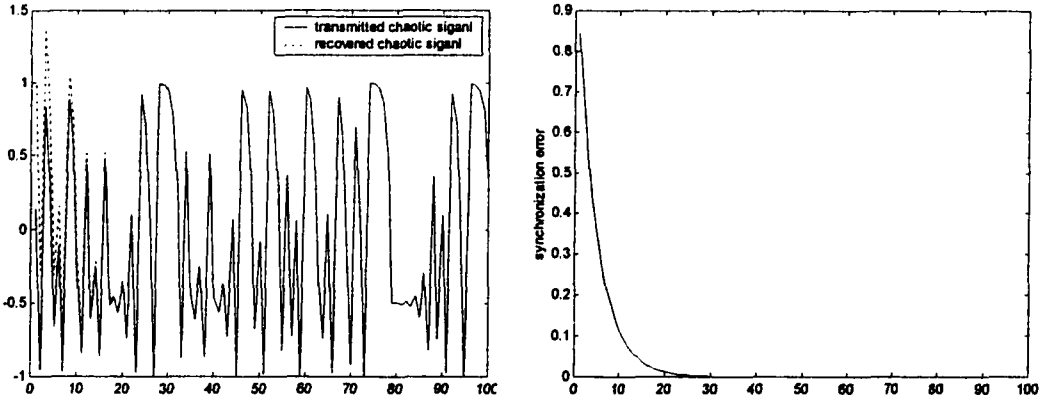

(a) (b)

Figure 4.5. Synchronization performance of the chaotic synchronization system under the noise free condition. (a) The transmitted and recovered chaotic signals and (b) the synchronization error.

4.3 Effect of higher transmission data rate

With an increasing amount of information to be transmitted, high data rate transmission is of great concern to current communication system design. The effect of transmission data rate on these chaos based communication systems is investigated in this subsection. We still assume the channel model to be AWGN. The same system parameters are used except that the transmission data rate f_b is increased from 50 *kbps* to 500 *kbps* and 1 *Mbps* for the high data rate investigation, which are the transmission speed achieved in the wireless local area network (WLAN) and cable communications. The bit duration T_b is therefore reduced to 2 μs and 1 μs, respectively. Note that the chaotic signal generation rate f_x remains at $f_x = 10\ MHz$. Figure 4.6 shows the model of the transmitted signal that is used to represent the higher transmission data rate in this study. We can see that the processing gain G of the system changes accordingly with different transmission rates. This implies that the samples of chaotic signals generated within each bit duration or the samples of chaotic signals to be transmitted to represent one data symbol are reduced with a higher data rate.

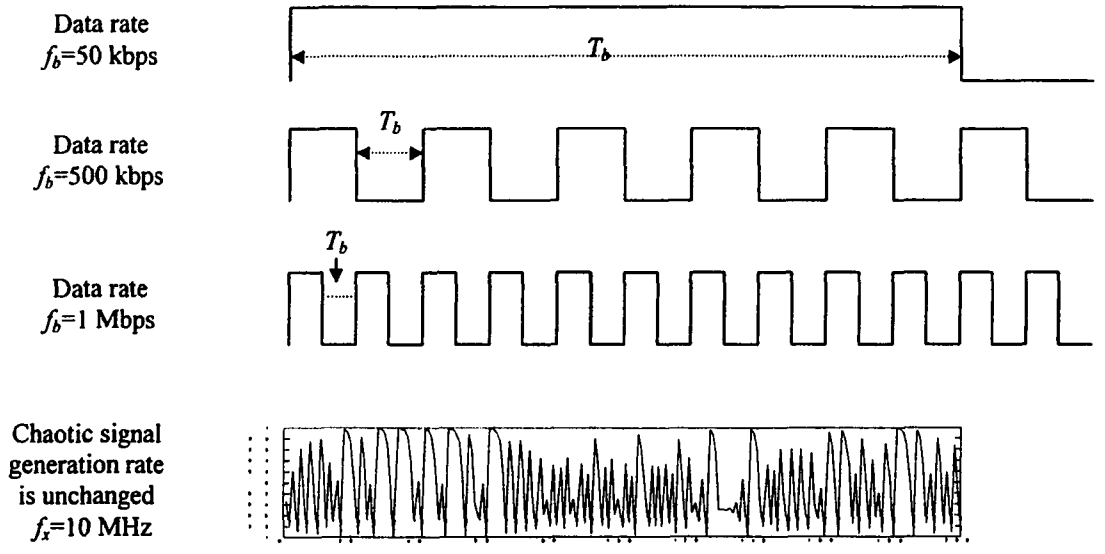

Figure 4.6. Model of the transmitted signal with higher transmission data rate.

The BER performances of all the chaos based schemes with $f_b = 500\ kbps$ and $f_b = 1\ Mbps$ are shown in Figures 4.7 and 4.8. Apparently, the BER performances of the NCSK, CCSK, CM and AF-CPM are deteriorated seriously by higher data rate transmission. For NCSK, its decision should be based on the difference of the bit energies of the received signal associated with the different transmitted digital symbols. In conventional modulation schemes using periodic basis functions, the signal *x(t)* is periodic with a periodicity of T_b, $\int_{T_b} x(t)^2 dt$ is therefore a constant. By contrast, chaotic signals are inherently non-periodic, so $\int_{T_b} x_i(t)^2 dt$ varies from one sample function of T_b to another. This effect results the non-zero variance in the observations of bit energies of chaotic signal in Figure 4.9. These bit energies are not exactly constant even in the noise-free condition over the duration of T_b. With a larger T_b, the estimated bit energies will have a smaller estimation variance as shown in Figure 4.9(a). It also shows that with a higher data rate transmission, the NCSK demodulation is much easier to be affected by the channel noise.

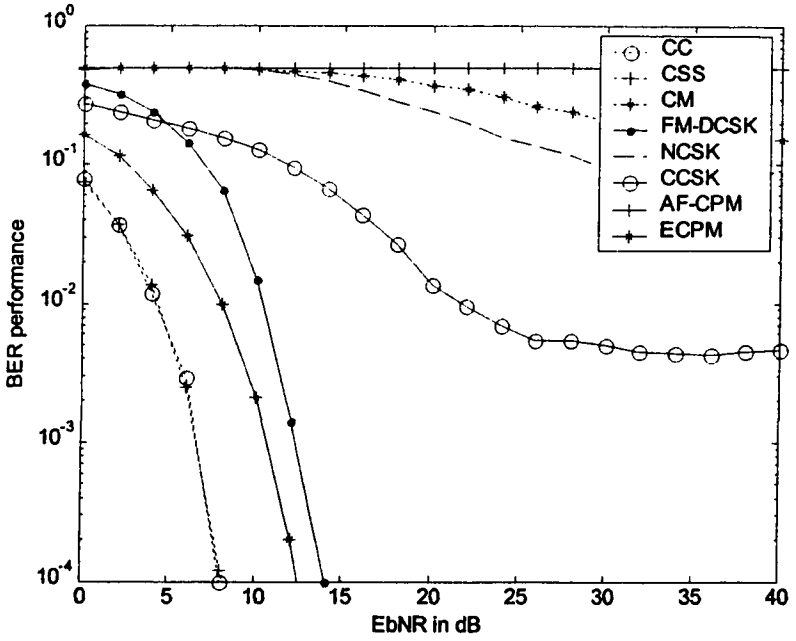

Figure 4.7. Noise performance of various chaos based scheme with data rate is $f_b = 500\ kbps$.

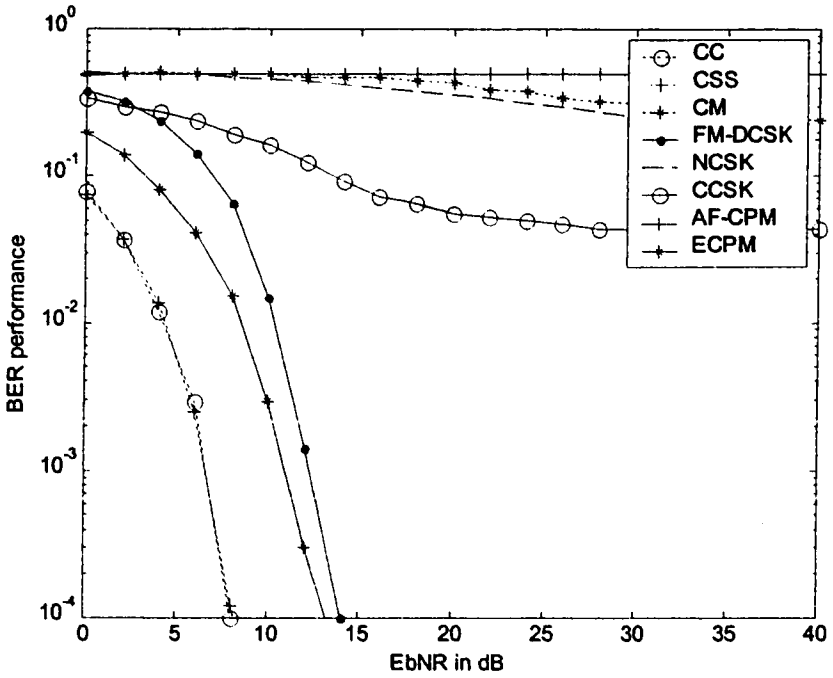

Figure 4.8. Noise performance of various chaos based scheme with data rate is $f_b = 1$ Mbps.

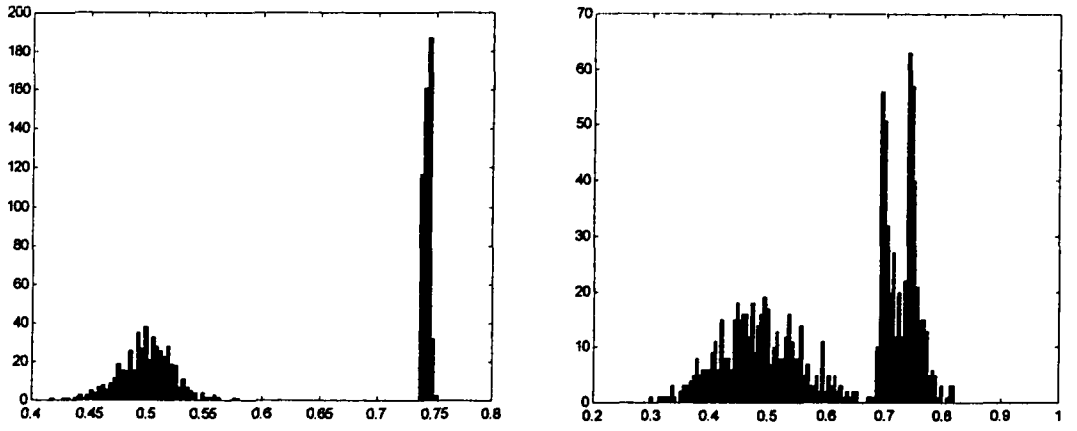

(a) (b)

Figure 4.9. Histogram plots of the observed bit energies at the output of the demodulator of NCSK in a noise free environment with (a) $T_b = 2$ μs, and (b) $T_b = 1$ μs.

For CM and CCSK, both of them require the operation of chaotic synchronization. Since a synchronization process needs a certain time period for convergence as shown in Figure 4.5, their performances are strongly dependent of the allowed time period for processing. By increasing the data rate, which in turn reducing the bit duration, the performance therefore gets worse. In addition, the noise component in (2.7) of the CM demodulation process, i.e, $\frac{1}{T_b}\int_0^{T_b} n(t)dt$, is also affected by the bit duration. The variance of this asymptotic estimation within a finite time period for an AWGN process can be derived as

$$\text{var}[\frac{1}{T_b}\int_0^{T_b} n(t)dt] \approx \frac{N_0}{T_b}. \tag{4.5}$$

When T_b is decreased or the data rate is increased, the variance in (4.5) also increases and hence results in a larger decision error. Based on our analysis, the performance of CM is even worse than that of CCSK.

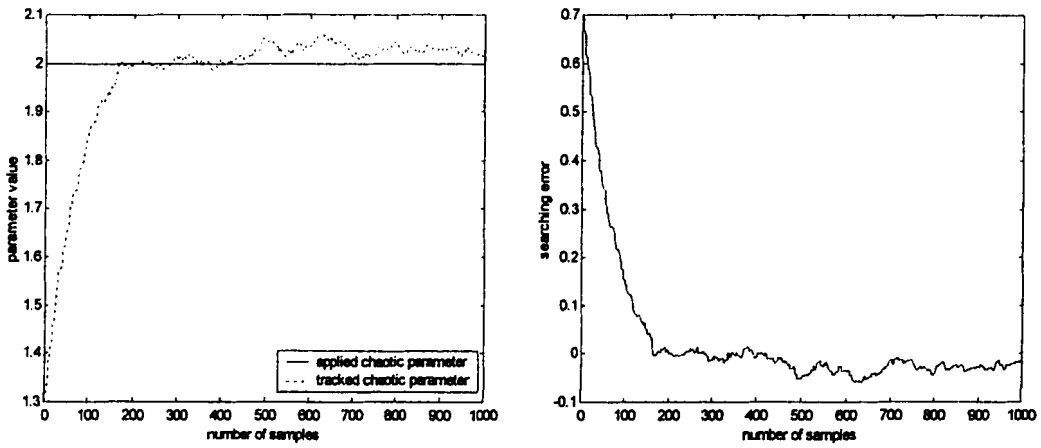

(a) (b)

Figure 4.10. Performance analysis of the chaotic parameter tracking based on the gradient search method for SNR ≈ 20 dB. (a) The convergence of the chaotic parameter of the Chebyshev map and (b) the corresponding tracking error.

The demodulator used in AF-CPM usually requires a relatively long sequence for convergence. As shown in Figure 4.10, the gradient based adaptive filter needs about 200 points to achieve the convergence. When data rate is increased as shown in Figures 4.7 and 4.8, the bit duration is too short and the signal sequence is not long enough for the adaptive filter to achieve the final convergence. The performance of AF-CPM is therefore degraded by using a higher data transmission rate.

From Figures 4.7 and 4.8, higher data transmission rate does not seem to have a strong impact on CC, CSS and FM-DCSK. The analytical BER performances of these schemes have already been reported individually in [1] and [45] which show their BER are not really related to the processing gain of the system. A higher data rate has little effect on the autocorrelation if the energy per bit is fixed in the system. The performances of these schemes are therefore not degraded [46].

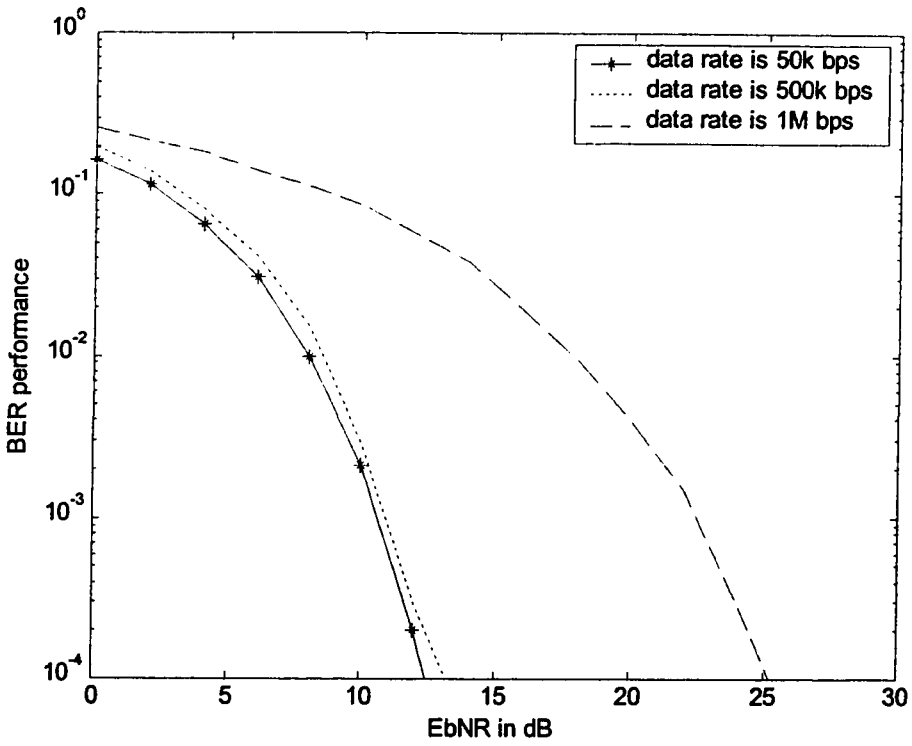

Figure 4.11. Noise performance of ECPM with different data rate f_b = 50 kbps, f_b = 500 kbps and f_b= 1 Mbps separately.

The performance of ECPM in Figures 4.7 and 4.8 are slightly different. In order to illustrate the affection of data rate clearly, we plot the performance of ECPM with different transmission data rate in Figure 4.11. The performances of ECPM with data rate $f_b = 50\,kbps$, $f_b = 500\,kbps$ and $f_b = 1\,Mbps$ are plotted together. Obviously, we observe that the performance of the ECPM with $f_b = 500\,kbps$ is only degraded by about 0.2 dB at BER = 10^{-3} than that of $f_b = 50\,kbps$. When the data rate is increased to 1 Mbps, the degradation is much more significant. Its performance is about 12 dB worse than that of $f_b = 500\,kbps$. According to the demodulation of ECPM in (3.11), the decision is dependent on both of the noise component $\frac{1}{T_b}\int_{T_b} n(t)dt$ and the information component $\frac{1}{T_b}\int_{T_b} x'(t)dt$. As indicated in (4.5), the estimation variance of the noise component is affected by the bit duration, and as the same, the estimation variance of the information component is also affected by the bit duration. That is,

$$\mathrm{var}[\frac{1}{T_b}\int_{T_b} x'(t)dt] \approx \frac{\delta_x^2}{T_b}. \tag{4.6}$$

Its noise performance therefore degrades while increasing the data rate. From our simulation results, the increment of the transmission data rate does not affect the performance of ECPM as serious as on the other schemes like NCSK, CCSK, CM and AF-CPM. Within a certain data rate range, at least for both data rate of 50 kbps and 500 kbps, the performance of ECPM still outperforms over FM-DCSK.

4.4 Effect of synchronization error

In a communication system, a coherent demodulator is one that requires a local carrier reference whose phase is an exact replica of or a close approximation to that of the incoming carrier. Furthermore, the output of a demodulator must be sampled periodically in order to recover the transmitted information. Since the propagation delay from the transmitter to the receiver is generally unknown at the receiver, the symbol timing must be retrieved. The process of generating carrier and timing references at the receiver is referred as synchronization [43, 48].

The synchronization problem can be described by developing a mathematical model for the signal at the input to the receiver. We assume that the communication channel produces a delay on the transmitted signal and corrupts it by some additive Gaussian noise. That is,

$$r(t) = s(t-\tau) + n(t), \tag{4.7}$$

where $s(t) = \mathrm{Re}[x'(t)e^{j2\pi f_c t}]$, τ is the propagation delay, $x'(t)$ is the equivalent lowpass chaotically modulated signal, and f_c is the central frequency of the RF channel. The received signal can also be expressed as:

$$\begin{aligned} r(t) &= \mathrm{Re}\left\{\left[x'(t-\tau)e^{j\phi} + z(t)\right]e^{j2\pi f_c t}\right\} \\ &= s(t,\tau,\phi) + n(t), \end{aligned} \tag{4.8}$$

where $\phi = e^{-2\pi f_c \tau}$ is the carrier phase distortion and $z(t)$ denotes the baseband equivalent channel noise. In a practical communication system, both τ and ϕ have to be estimated for the demodulator to detect the received message coherently. There are basically two criteria that are widely applied to synchronization: the maximum-likelihood (ML) and

maximum a posteriori probability (MAP). Note that synchronization techniques based on these criteria might vary a lot, depending on the modulation schemes employed and the degree of accuracy desired [1].

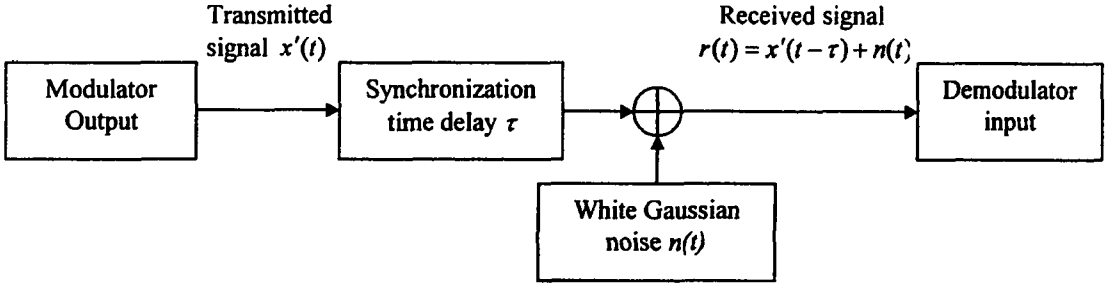

Figure 4.12. The channel model of the non-ideal system with propagation delay of the received signal passed through an AWGN channel.

To understand the effect of synchronization error on these chaos based communication schemes, we consider communication systems without applying any additional synchronization procedure. The ability of these chaotic schemes in overcoming synchronization errors will be evaluated in this subsection. In our study, the RF frequency is considered to have been removed completely and hence the synchronization problem is caused by the propagation delay τ only, as shown in Figure 4.12. That is,

$$r(t) = x'(t-\tau) + n(t). \tag{4.9}$$

In the above model, the synchronization error τ is generated by using a zero mean Gaussian random process as shown in Figure 4.13. The probability density function of τ is given by

$$P_f(\tau) = \frac{1}{\sqrt{\pi T_b}} \exp[\frac{-\tau^2}{T_b}]. \tag{4.10}$$

It has a zero mean, and the maximum synchronization error is $T_b/2$ relative to each bit duration T_b. The estimation error of τ is usually required to be a relatively small fraction of T_b, say about ±1% of T_b in practical applications. The synchronization error caused by the above propagation delay model is therefore of considerable amount to a digital communication system.

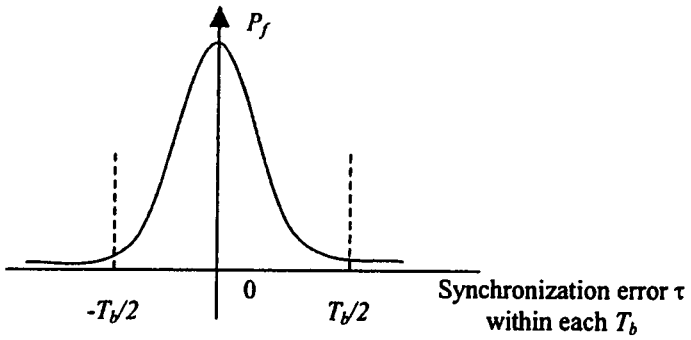

Figure 4.13. The distribution plot of the propagation delay within each bit duration T_b.

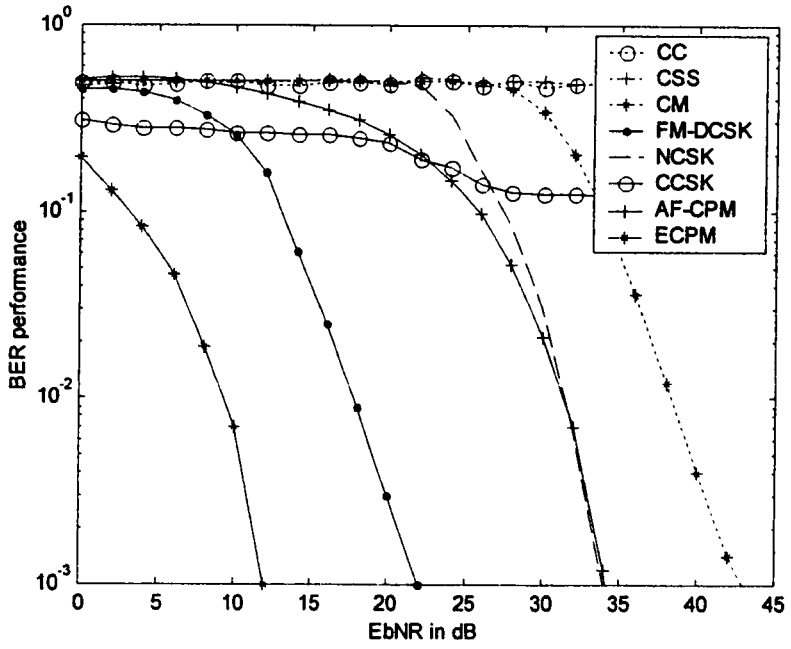

Figure 4.14. Effect of synchronization error on the various chaos based communication systems.

We plot the BER versus E_bNR of the various chaos based SS schemes with synchronization error in Figure 4.14. The data rate is set as $f_b = 50\,kbps$, and the bit duration T_b is equal to $20\,\mu s$. The outputs of the demodulator for CSS and CC are based on coherent correlation. That is,

$$m = \int_0^{T_b} x'(t-\tau)x(t)dt\,. \tag{4.11}$$

The existence of the delay τ makes the reference signal $x(t)$ and the received signal $x'(t-\tau)$ almost uncorrelated. The output m is therefore almost identical to zero, and the

receiver fails to determine the transmitted data symbol. As in the conventional DSSS system, CSS and CC cannot operate properly if the system loses synchronization. In this case, an additional synchronization procedure must be implemented.

The performance of CCSK also deteriorates seriously in the existence of synchronization error. In the demodulator, the received delayed signal is used to drive the chaotic synchronization system, and the correlation is performed between the delayed signal and the recovered delayed signal $x_r(t-\tau)$ as shown below:

$$m_i = \int_0^{T_b} x'(t-\tau)x_{i,r}(t-\tau)\,dt \quad i=0,1. \tag{4.12}$$

A considerable amount of synchronization error will drive the chaotic synchronization system out of convergence within each bit duration. Therefore, the observed outputs, m_0 and m_1, of two correlators become too close for an accurate detection on the transmitted data symbol.

For the effect of the delay τ on FM-DCSK and NCSK, we consider their self-correlation based demodulators

$$\begin{aligned} m &= \int_{T_b/2}^{T_b} x'(t-\tau)x'(t-T_b/2-\tau)dt \\ &= \int_{T_b/2+\tau}^{T_b+\tau} x'(t)x'(t-T_b/2)dt \end{aligned} \quad \text{for FM-DCSK} \tag{4.13}$$

$$\begin{aligned} m &= \int_0^{T_b} x'(t-\tau)x'(t-\tau)dt \\ &= \int_{\tau}^{T_b+\tau} x'(t)x'(t)dt \end{aligned} \quad \text{for NCSK} \tag{4.14}$$

The propagation delay τ causes the correlation window to be shifted by some time interval. Within the "shifted" correlation window, these demodulators can still operate properly. From Figure 4.14, FM-DCSK degrades about 10 dB at BER = 10^{-3} level, and NCSK seems to degrade about 2 dB. From (2.4) we know that the demodulation process of FM-DCSK is based on the self-correlation within each half bit duration $T_b/2$. In our synchronization error model, the synchronization delay is distributed within [0, $T_b/2$], which almost spans the whole decision period of FM-DCSK. For FM-DCSK, this amount of synchronization errors is relatively serious. If we reduce the propagation delay range to [0, $T_b/4$] as shown in Figure 4.15, then its performance is degraded only by 5 dB at BER = 10^{-3}.

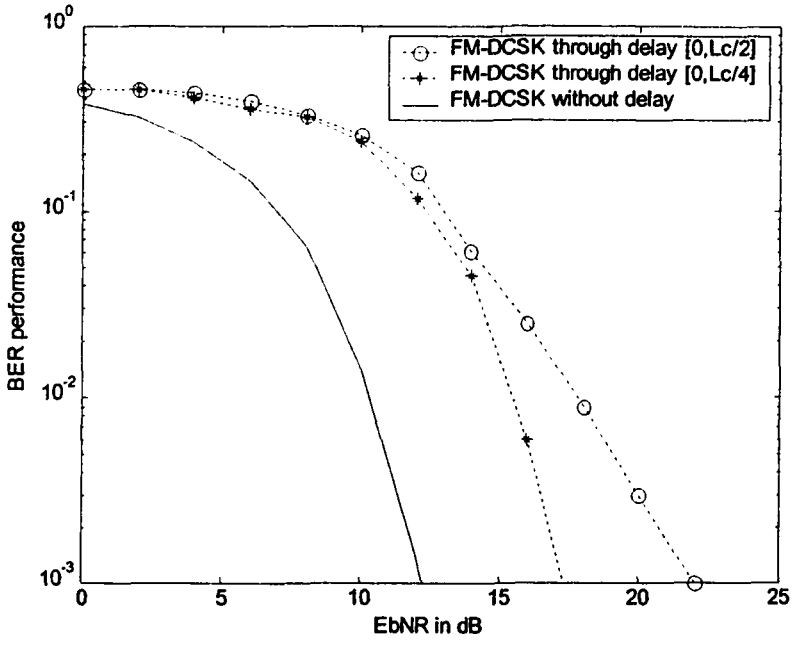

Figure 4.15. Performance of FM-DCSK through propagation delay channel with different delay ranges.

For those systems such as ECPM, AF-CPM and CM that do not employ a correlator for demodulation, the propagation delay τ causes a delay of the sampling timer at their demodulation output and hence the effect is that the demodulation output is sampled at time instant $nT_b+\tau$ instead of nT_b. For instance, the output of the ECPM system is given as:

$$m = \int_0^{T_b} x'(t-\tau)dt = \int_{\tau}^{T_b+\tau} x'(t)dt. \qquad (4.15)$$

This shifting in time does not really cause much error to the demodulators, and their performances therefore remain almost unchanged even under such a large propagation delay.

In conclusion, most of the chaotic modulation methods except for CCSK are robust to the synchronization problem of carrier and symbol delay. This robustness property makes chaotic modulation in favour of the spreading code SS approach and suitable for communications in environments with serious propagation delay and inaccurate timing setting between transmitter and receiver. One of such environments is the multipath channel to be discussed in the next subsection.

4.5 Multipath channels

In many applications such as WLAN, mobile phones and indoor radio, there is usually more than one path from transmitter to receiver in the radio channel. The received signal therefore contains components that have travelled from the transmitter to the receiver through multiple propagation delay paths. This radio channel is called multipath channel [1,43,48], and is a key consideration for wireless communications.

The performances of all these chaos based communication systems operated through a multipath channel are evaluated by using a model given in Figure 4.16 [16,43]. This time-invariant multipath model is assumed to have N propagation paths. The signal received at the receiver is the summation of components transmitted through all these N paths with delay τ_p and power attenuation a_p. That is

$$r(t) = \sum_{p=0}^{N-1} a_p s(t-\tau_p) + n(t). \tag{4.16}$$

The symbol p denotes the pth propagation path. The effect of the multipath channel on a transmitted signal is represented by its lowpass equivalent signal $r_l(t)$:

$$r_l(t) = \sum_{p=0}^{N-1} a_p e^{-j2\pi f_c \tau_p} x'(t-\tau_p) + n(t), \tag{4.17}$$

where f_c is the RF central frequency and $x'(t)$ is the lowpass equivalent modulated signal. It follows that the equivalent low pass multipath channel is described by the time-invariant impulse response

$$c(\tau,t) = \sum_{p=0}^{N-1} a_p e^{-j2\pi f_c \tau_p} \delta(\tau-\tau_p). \tag{4.18}$$

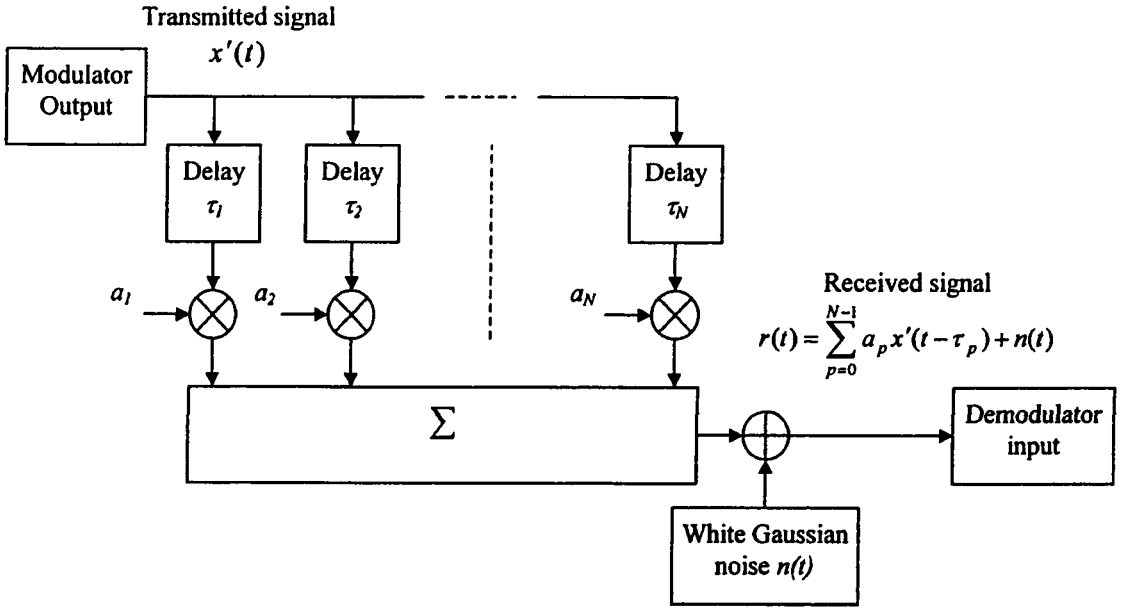

Figure 4.16. Propagation delay model of a multipath channel with additive white Gaussian noise.

In this time-invariant multipath model, the attenuation factor a_p and time delay τ_p are assumed to be unchanged with time but are different for each path. $f_c \cdot \tau_p$ determines the phase shift of the signal transmitted from different propagation paths. The autocorrelation function $\phi_c(\tau)$ is defined as

$$\phi_c(\tau_p) = \frac{1}{2} E[c^*(\tau_p, t) \cdot c(\tau_p, t)], \tag{4.19}$$

and it is simply the average power output of each propagation path as a function of the time delay τ. For this reason, it is called the multipath intensity profile or the delay power spectrum of the channel. Typically, the measured multipath intensity profile $\phi_c(\tau)$ may appear as shown in Figure 4.17 and can be given as a function of τ given by

$$\phi_c(\tau) = P_{ave} \cdot \exp(-2\pi \frac{\tau}{T_m}), \tag{4.20}$$

where P_{ave} is the average signal power in the direct path. The range of values of τ over which $\phi_c(\tau)$ is essentially nonzero is called the multipath spread, denoted as T_m. The multipath spread is defined as the difference between the longest and the shortest path delays [1], that is,

$$T_m = \tau_{max} - \tau_{min}. \tag{4.21}$$

Usually, the shortest path points to the direct path where there is no propagation delay, thus $\tau_{\min} = 0$ and $T_m = \tau_{\max}$.

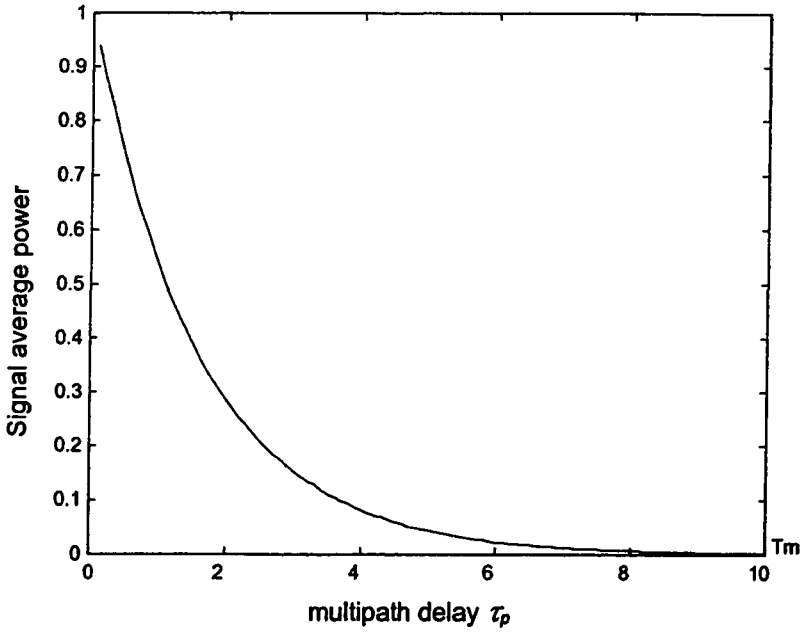

Figure 4.17. Multipath intensity profile illustration for different propagation delays paths.

In our simulation model, the following parameters are used: $f_b = 50\ kbps$, $T_b = 20\ \mu s$, $T_x = 0.1\ \mu s$, $T_m = \frac{T_b}{2} = 10\ \mu s$, and N=11 propagation paths in the channel model including the direct path. The time delay difference between two adjacent paths is defined as

$$\Delta\tau = \left|\tau_{p+1} - \tau_p\right| = \frac{T_m}{N-1}. \tag{4.22}$$

In this model, $\Delta\tau = 1\ \mu s$. The BER performances of all the chaotic communication schemes based on this multipath model are shown in Figure 4.18.

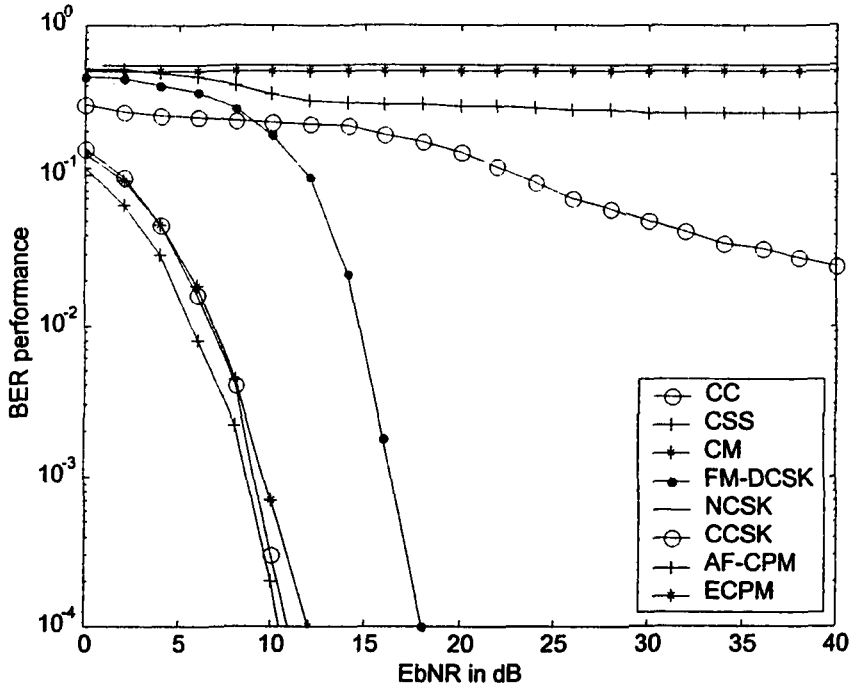

Figure 4.18. BER performance of the different chaos based communication systems in a multipath channel.

Apparently, four of these chaos communication schemes: CCSK, NCSK, CM and AF-CPM, fail to operate normally in this multipath channel. Their BER performances are completely deteriorated. Since the signals from the undirect paths act like noise to the demodulation process, the synchronization system in CCSK and CM and the adaptive filter in AF-CPM cannot handle this extra huge amount of noise. Therefore, they fail to retrieve the transmitted data symbols from the direct path. The problem with NCSK is that the threshold used in the detection process is related to the system SNR level. However, in a multipath channel, the received signal to noise ratio is changed accordingly to the channel model. In this case, the threshold value has to be adjusted on-time according to the channel model for a satisfactory performance.

For CSS and CC, correlation is performed between the received signal and the coherent reference signal. It means that signals from all paths will be multiplied with the reference signal. That is,

$$
\begin{aligned}
m &= \int_0^{T_b} r(t)x(t)dt \\
&= \int_0^{T_b} \left\{ \sum_{p=0}^{N-1} a_p x'(t-\tau_p) + n(t) \right\} x(t)dt \\
&= \int_0^{T_b} a_0 x'(t)x(t)dt + \int_0^{T_b} \sum_{p=1}^{N-1} a_p x'(t-\tau_p)x(t)dt + \int_0^{T_b} n(t)x(t)dt.
\end{aligned}
\tag{4.23}
$$

Since those signals coming from undirect paths $x'(t-\tau_p)$ are almost uncorrelated with the reference signal *x(t)*, we have $\int_0^{T_b} \sum_{p=1}^{N-1} a_p x'(t-\tau_p)x(t)dt \approx 0$. In other words, the signals from undirect paths are removed by the correlator during the demodulation process. In our time-invariant multipath channel, a_0 is a constant (= 1) and is almost unchanged. The system can therefore retrieve the transmitted symbols from the direct path signal. Thus, CSS and CC can operate well under the multipath channel with a 0.5 dB degradation at BER = 10^{-3}.

The performance of FM-DCSK under multipath channel has been investigated in [16]. According to Figure 4.18, the degradation is about 5 dB at BER = 10^{-3}. Its complicated output from the self-correlation based demodulator is

$$
\begin{aligned}
m &= \int_{T_b/2}^{T_b} r(t)r(t-T_b/2)dt \\
&= \int_{T_b/2}^{T_b} a_0{}^2 x'(t)x'(t-T_b/2)dt + \sum_{p=1}^{N-1} X_p X_p + \sum_{p\neq q} X_p X_q + \tilde{N},
\end{aligned}
\tag{4.24}
$$

where $X_p X_p = \int_{T_b/2+\tau_p}^{T_b+\tau_p} a_p{}^2 x'(t)x'(t-T_b/2)\,dt$ is the self-correlation of the signals from undirect paths, $X_p X_q = \int_{T_b/2}^{T_b} a_p a_q x'(t-\tau_p)x'(t-T_b/2-\tau_q)]\,dt$ is the correlation between signals from every two different paths, and $\tilde{N} = \int_{T_b/2}^{T_b} \left\{ \sum_{p=0}^{N-1} a_p [x'(t-\tau_p)n(t-T_b/2) + x'(t-T_b/2-\tau_p)n(t)] \right\} dt$ is the channel noise component. Obviously, $X_p X_q$ and $\tilde{N}$ are basically noise to the detection. $X_p X_q$ is in the same format as the synchronization error discussed in the previous subsection.

Another scheme that is robust to the multipath effect is ECPM. Considering the output of the ECPM demodulator:

$$
\begin{aligned}
m &= \int_0^{T_b} r(t)dt \\
&= \int_0^{T_b} \left\{ \sum_{p=0}^{N-1} [a_p x'(t-\tau_p)] + n(t) \right\} dt \\
&= \int_0^{T_b} a_0 x'(t)dt + \sum_{p=1}^{N-1} \int_{\tau_p}^{T_b+\tau_p} a_p x'(t)dt + \int_0^{T_b} n(t)dt,
\end{aligned}
\tag{4.25}
$$

we observe that the only distortion caused by multipath channels is in the second component $\sum_{p=1}^{N-1} \int_{\tau_p}^{T_b+\tau_p} a_p x'(t)dt$. It is the summation of the estimation mean values of the signals coming from undirect paths and can also be treated as estimation of the signal in the direct path with power attenuation by employing a time (τ_i) shifting window. Since ECPM is extremely robust to synchronization errors, it is not surprising to observe that ECPM is not sensitive to the multipath effect either. From the second component, we can also see that if a_p is a positive value, the second component will give a positive affection on the demodulation, which means the decision will not be distorted. However, if a_p is negative, the result will generate a negative affection on the detection since it will change the sign of the estimated mean value of the transmitted chaotic signal. Passing through the multipath channel model used in our study, ECPM shows almost unaffected from the noise component. It is a little worse than that of CC and CSS under multipath channel. This makes it good substitution to the conventional DSSS system under multipath environment and superior to other chaotic schemes.

CHAPTER 5

APPLICATION OF ECPM TO SS ANALOG COMMUNICATIONS

5.1 Introduction

Among current applications of SS techniques, most of them are based on the digital scheme. The increasing development toward digital communication is mainly because that it has flexibility in digital formats and can achieve much better transmission quality than an analog communication system [1,2,48]. However, in most communication applications, information to be transmitted is inherently analog in nature, such as speech, audio, video and radar signals [49,50]. In addition, most encountered transmission channels are also analog channels, for example, the AWGN channel, where, in practice, the Shannon theorem does not apply well. Under these conditions, the heart of any digital communication system is to convert the analog signal into digital formats by scaling, sampling and quantization. But the typical analog-to-digital conversion (ADC) and digital-to-analog conversion (DAC) processes in a digital coding scheme not only produce the well-know quantization noise, but generate harmonic and intermodulation products. Thus its performance depends crucially on being able to choose the proper quantization schemes and quantization levels [51-53].

Recently, there has been a resurgence of interest in analog communication or partially analog approaches in the form of digital techniques [35]. It is not surprising to see that the ECPM scheme can operate well not only for digital communications but for analog communications as well. The ability for transmitting in both digital and analog formats makes ECPM even more attractive. With the mean value estimation technique as the demodulator in the digital ECPM scheme, the objective of demodulation is to tell the difference between two discrete parameter values. However, in the analog scheme, the goal of the demodulation is to estimate the parameter values distributed in the whole chaotic regime.

5.2 System structure of analog ECPM scheme

In the analog ECPM system, the analog information signal *s(t)* is modulated directly into the chaotic system (3.7) by

$$x(t) = f_{g(s(t))}(\mathbf{x}(t-1)). \tag{5.1}$$

The chaotic parameter θ is modulated according to the transmitted information signal *s(t)* by the parameter modulation function $g(\cdot)$, that is $\theta(t) = g(s(t))$. After modulation, the chaotic parameter is an analog signal $\theta(t)$ continuously distributed on the whole chaotic regime rather than on two discrete parameter values, θ_0 and θ_1 as in the digital ECPM scheme. Based on the time-variant parameter $\theta(t)$, the chaotic system is controlled by the frequency f_x to generate the wideband chaotic signal. The controlling frequency f_x of the chaotic signal should be much larger than the frequency f_i of the analog signal *s(t)* in order to achieve SS characteristics. That is $f_x >> f_i$. In other words, the generation rate of chaotic signal has to be much faster than the variation of the chaotic parameter. Usually, the controlling frequency f_x of the chaotic system is equal to the RF central frequency in a practical system.

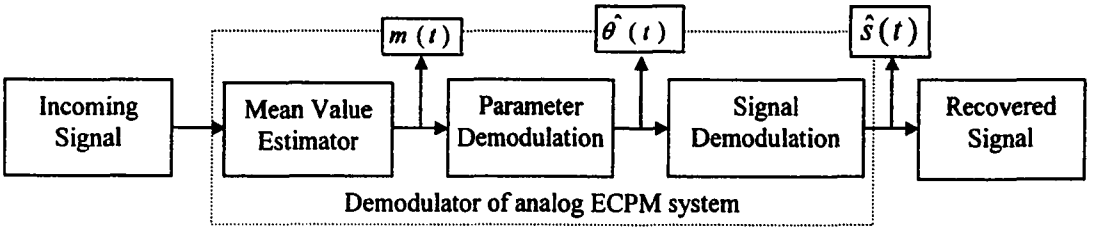

Figure 5.1. Block diagram of the demodulator of the analog ECPM system.

At the receiver, the mean value estimator is used to demodulate the analog information signal. Unlike its application in the digital scheme, where the bit duration T_b is set as the estimation window length and symbol timing synchronization is required, the demodulator is modified slightly as shown in Figure 5.1. For the mean value estimation module, we apply a moving window to estimate the mean value of the incoming baseband signal $r(t) = x(t) + n(t)$ in an online fashion. At the output of the mean value estimator, we have a continuous output signal *m(t)*, which can be expressed by the following equation:

$$
\begin{aligned}
m(t) &= \frac{1}{T_w}\int^{+T_w} r(t)dt \\
&= \frac{1}{T_w}\int^{+T_w} x(t)dt + \frac{1}{T_w}\int^{+T_w} n(t)dt \\
&= \hat{M}(\theta(t)),
\end{aligned}
\tag{5.2}
$$

where T_w is the length of the moving window of the mean value estimator. In order to achieve the characteristics of the SS transmission, the window length T_w has to meet the following requirement, that is

$$T_s \geq T_w > T_x, \tag{5.3}$$

where $T_s = \frac{1}{f_s}$ and f_s is the sampling rate of the analog signal. According to the Nyquist sampling theory, the sampling rate must be greater than twice of the frequency of the signal, $f_s > 2f_i$. The criterion of $T_s \geq T_w$ ensures the demodulator to recover the transmitted analog signal effectively and correctly without losing any information. The step size between two adjacent chaotic states, $T_x = \frac{1}{f_x}$ can be considered as the chip duration in a SS communication system. The ratio of T_w to T_x is the processing gain G in a SS analog communication system. That is, $G = \frac{T_w}{T_x}$. If the processing gain is large enough, we have $m(t) = \hat{M}(\theta(t)) \approx M(\theta(t))$. Passing through the mean value estimator, the noise component in the signal *m(t)* is $\frac{1}{T_w}\int^{+T_w} n(t)dt$ which is approximately equal to zero. In fact, the power of the channel noise has been suppressed by G times after the demodulation. As discussed in Theorem 3 in subsection 3.1, the estimator has the estimation variance of $\frac{\delta_x^2 + \delta_n^2}{G}$. This affects the recovery performance of this analog transmission.

For the analog ECPM system, the chaotic system is required to have a strictly mono tone mean value function. From the output of the mean value estimator, we can then demodulate the chaotic parameter according to the mean value function of the

chaotic signal. This process is called parameter demodulation in Figure 5.1 and can be expressed by the following equation:

$$\begin{aligned}\hat{\theta}(t) &= M^{-1}(m(t)) \\ &\approx M^{-1}(M(\theta(t))).\end{aligned} \tag{5.4}$$

If the exact form of the mean value function is not available, we can employ the gold search method [44] to find the mapped parameter.

Once the transmitted chaotic parameter is estimated, the transmitted analog signal can be determined from the output signal of $\hat{\theta}(t)$ according to the parameter modulation function $g(\cdot)$. Such process is called signal demodulation in Figure 5.1. That is

$$\hat{s}(t) = g^{-1}(\hat{\theta}(t)). \tag{5.5}$$

In practical communication applications, the parameter modulation function $g(\cdot)$ can be set as a linear function $\theta(t) = g(s(t)) = as(t) + b$. In this case, (5.5) can be simply expressed as $\hat{s}(t) = g^{-1}(\hat{\theta}(t)) = \frac{\theta(t) - b}{a}$. For secure communications, more complicated functions can be used for the parameter function $g(\cdot)$ to perform encryption, because the transmitted analog signal cannot be decoded without the knowledge of $g(\cdot)$.

5.3 Performance evaluation

The performance of the proposed analog ECPM SS communication system is investigated by transmitting various kinds of signals under the AWGN environment. A computer simulation model is built according to the practical communication system [49]. The detailed block diagram of the simulation model is shown in Figure 5.2.

The simulation model consists the following modules: the analog source generator, where various kinds of analog information signals are generated; the chaotic signal generator, where the Chebyshev map is used to generate the chaotic signal. The bifurcating parameter θ is modulated with the analog information within [1.3, 2] through the parameter modulation function; the RF modulation/demodulation parts, where DSB-AM/ADM is selected as the passband modulator/demodulator; the communication environment is supposed to be AWGN channel and the proposed demodulator including mean value estimator, parameter decoder and parameter demodulation function. An

integrator with a sliding window is used as the mean value estimator since it is computationally efficient. The length of the moving window T_w is adjusted according to the frequency of the analog signal and the required processing gain of the system. At the output of the demodulator, the continuous output signal is seen as the recovered information signal directly without applying any extra process. The transmission SNR level is adjusted by controlling the transmission power. Under different SNR conditions, the performance of the transmitted analog signal is evaluated by its recovery distortion: mean square error (MSE).

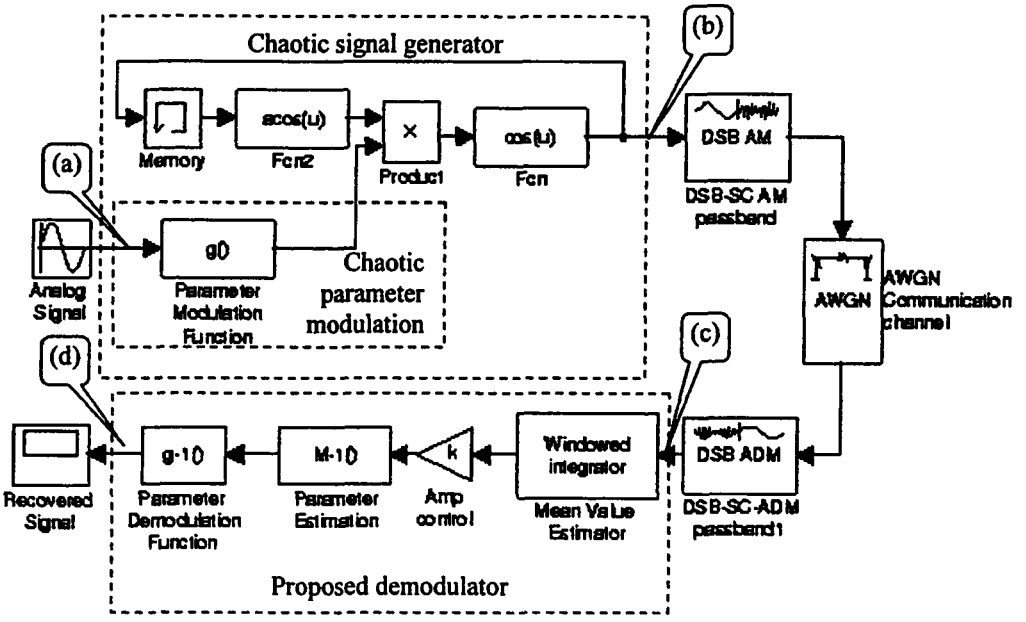

Figure 5.2. Detailed structure of the simulation model of analog ECPM system.

In our study, the following system parameters are used through the simulation model: RF carrier frequency: f_c=10 MHz, power spectrum density of the channel noisc: P_n=1, the controlling frequency of the chaotic system: f_x=10 MHz, processing gain G = 1000. The simulation model is designed to transmit the analog information signal directly, however, signals in both analog (continuous) and discrete formats can also be transmitted and recovered through this system without changing the simulation model.

In our fist experiment, a continuous sinusoidal wave signal is transmitted through the above model. The information signal is expressed as: $s(t) = \sin(2\pi f_i t)$, f_i= 1 kHz. In order to achieve a processing gain of 1000, the window length of the mean value

estimator in the demodulator is set as $T_w = G/f_x = 100\mu s$. The continuous signal is modulated into the chaotic parameter $\theta(t)$ by the parameter modulation function given by:

$$\theta(t) = 0.35s(t) + 1.65. \tag{5.6}$$

Thus the modulated parameter remains in the chaotic regime [1.3 2] and the transmission signal is wideband for SS communications. The modulated chaotic signal is transmitted after a DSB-AM modulation. The SNR of the noise corrupted signal transmitted through the AWGN channel and received at the antenna is controlled at 0 dB. That is,

$$SNR = 10\log_{10}\left(\frac{P_s}{P_n}\right) = 0\,dB. \tag{5.7}$$

The quality of the service (QoS) of an analog communication system is usually determined by normalized MSE, that is the ratio of the average distortion noise power to the average power of the recovered signal, expressed as $\frac{MSE}{P_{sr}}$, where P_{sr} denotes the average power of the recovered signal $\hat{s}(t)$ in (5.5) and MSE denotes the distortion power between the recovered signal and the original signal. That is,

$$MSE = \lim_{T\to\infty}\frac{1}{T}\int\left[s(t) - \hat{s}(t)\right]^2 dt. \tag{5.8}$$

In our study, only the MSE is used in the evaluation since the signal power is fixed. The signal waveforms processed in the different transmission stages through the system model are illustrated in Figure 5.3. Points (a)~(d) are labelled in the block diagram of the simulation model in Figure 5.2. The distortion between each samples of the original signal and the recovered signal is also shown here. It gives us a clear description on the operation process of the analog ECPM system. By observing the original sinusoidal waveform, recovered signal waveform and their distortions in Figure 5.3, we can see that the recovery performance of the transmitted continuous analog information signal is pretty good even at a very low SNR level.

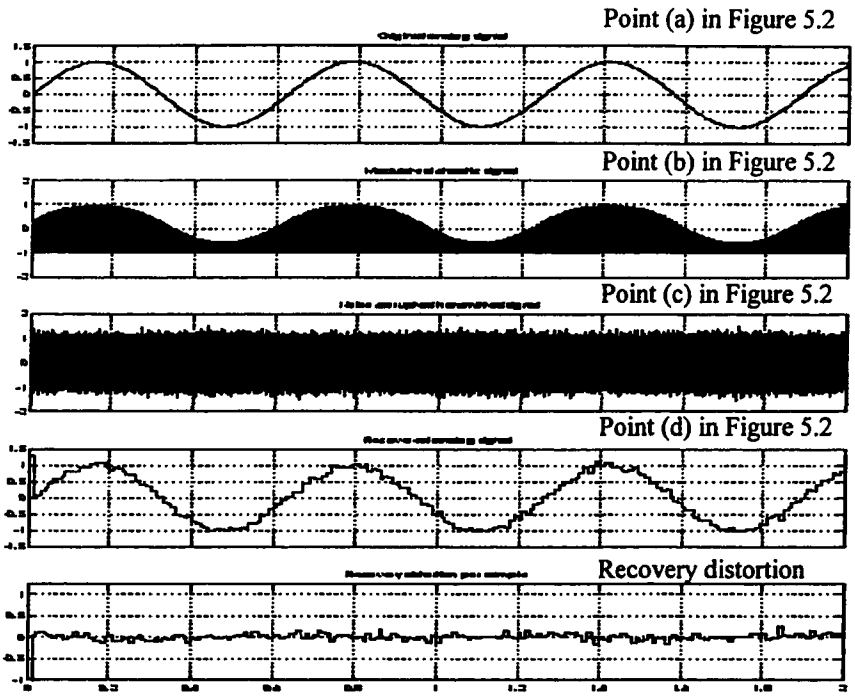

Figure 5.3. Signal waveforms in various stages of the proposed ECPM SS communication system.

The recovery performance of the analog ECPM system is shown in Figure 5.4. The performance is evaluated by plotting the recovery distortion MSE between the recovered signal and the original signal versus various levels of SNR. The range of SNR considered in our study is from –20dB to 20 dB with an increment of 2 dB. Each MSE value is computed by using an average of 1000 trials. Except the sinusoidal signal, a Gaussian random signal is also employed as a second information source for transmission. The Gaussian random signal is generated from the Gaussian random signal generator integrated in MATLAB. The generation rate is 1 kHz. The generated random signal distributes within [-1, 1] and it is modulated into the chaotic parameter by (5.5). The recovery performance of the Gaussian random signal is also plotted in Figure 5.4. From the figure we observe that even though the random signal is much more complicated than the sinusoidal signal, the ECPM analog system can recover both of them with a pretty good performance. The recovery performances for sinusoidal signal and random signal are very close. Both of them can achieve a recovery distortion of MSE $\approx$ 25 dB at SNR of 0 dB.

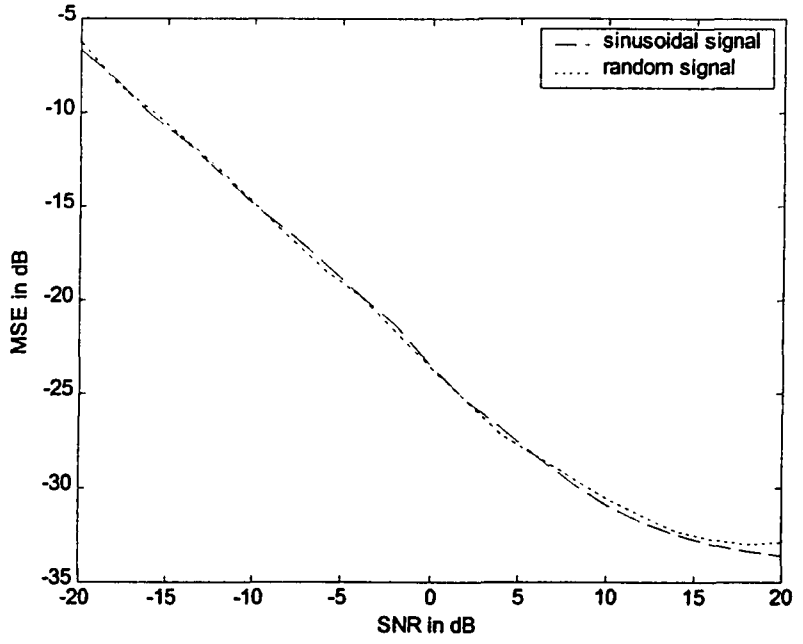

Figure 5.4. Recovery performance for sinusoidal signal and Gaussian random signal.

In the second experiment, two real multimedia signals, one is a speech signal and the other is an image, are transmitted and recovered by the analog ECPM system. A recorded male voice " *Welcome to Canada*" is used as the speech information message. The sampling frequency f_s of the speech signal is 22.05 kHz in our study. According to (5.3), we set the length of the mean value estimation window as $T_w = T_s = \frac{1}{f_s}$, that is $T_w = \frac{1}{22.05\ kHz} \approx 45\ \mu s$. In order to keep the processing gain of the system as 1000, the controlling frequency f_x of the chaotic system is fixed as 22.05 MHz. The speech signal is normalized within [-1, 1] first and then is modulated to the chaotic parameter according to (5.6). To clearly illustrate the recovery performance of the system, we plot the original voice signal, the noise corrupted voice signal and the recovered voice signal through the analog ECPM system in Figure 5.5. The illustrated noise corrupted signal is obtained under the transmission condition of $SNR = 0\ dB$. The recovery distortion under this transmission condition is $MSE = -25.657\ dB$. This MSE quality is well acceptable for speech communications. For the image signal, we employ an image of a little bridge as shown in Figure 5.6(a). The original image is saved in the "tif" format with a size of

256×256. The sampled signal, which is read from the "tif" file by the MATLAB function "*IMREAD*", are integers ranging between 0 and 255. This image signal is first normalized to [-1,1] and the normalized sequence is then modulated into the chaotic parameter by (5.6).

The recovered image is also saved as a ".tif" file. The original image, the noise corrupted image and the recovered image through the ECPM system are illustrated in Figure 5.6. The transmission condition is of $SNR = 0\ dB$ and the recovery distortion is $MSE = -25.448\ dB$. From Figure 5.6(c), we can see the quality of the recovered image is of good perceptual quality.

The MSE performances of the analog ECPM system for transmitting these multimedia signals are plotted in Figure 5.7. Their recovery performances are quite similar.

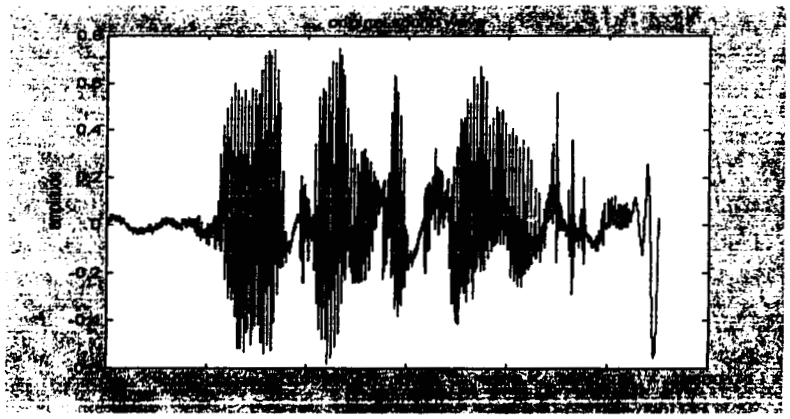

(a) Original sound wave

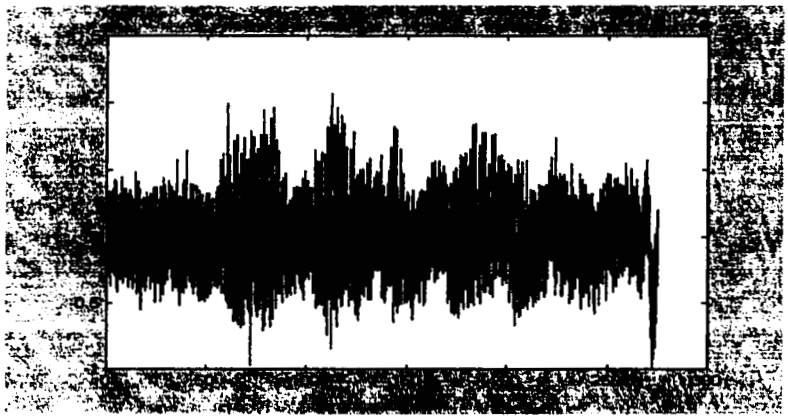

(b) Noise corrupted sound wave

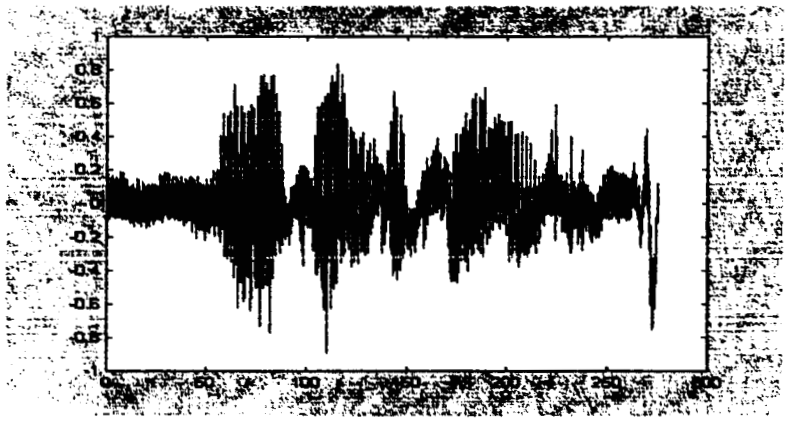

(c) Recovered sound wave

Figure 5.5. Recovery performance of the speech signal through the proposed ECPM SS analog communication system. SNR = 0 dB, processing gain G = 1000, recover quality MSE = -25.657 dB.

(a) Original image

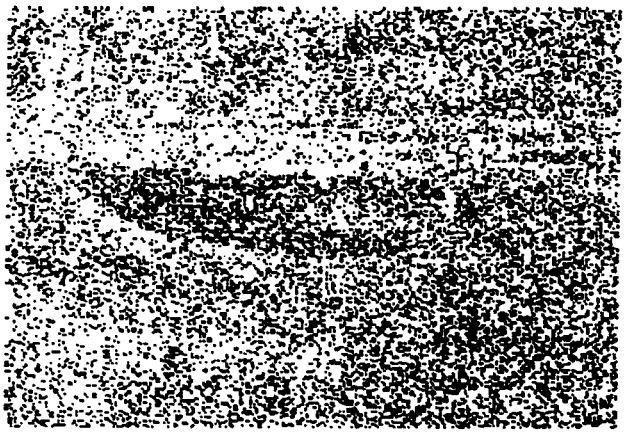

(b) Noise corrupted image

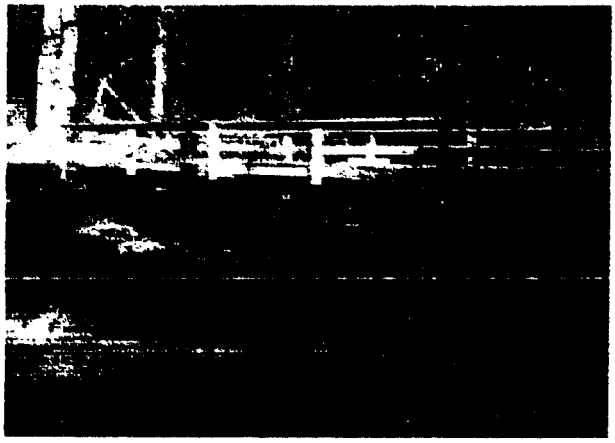

(c) Recovered image

Figure 5.6. Recovery performance of the image signal through the proposed ECPM SS analog communication system, SNR = 0 dB, processing gain G = 1000, recover distortion MSE = -25.448dB.

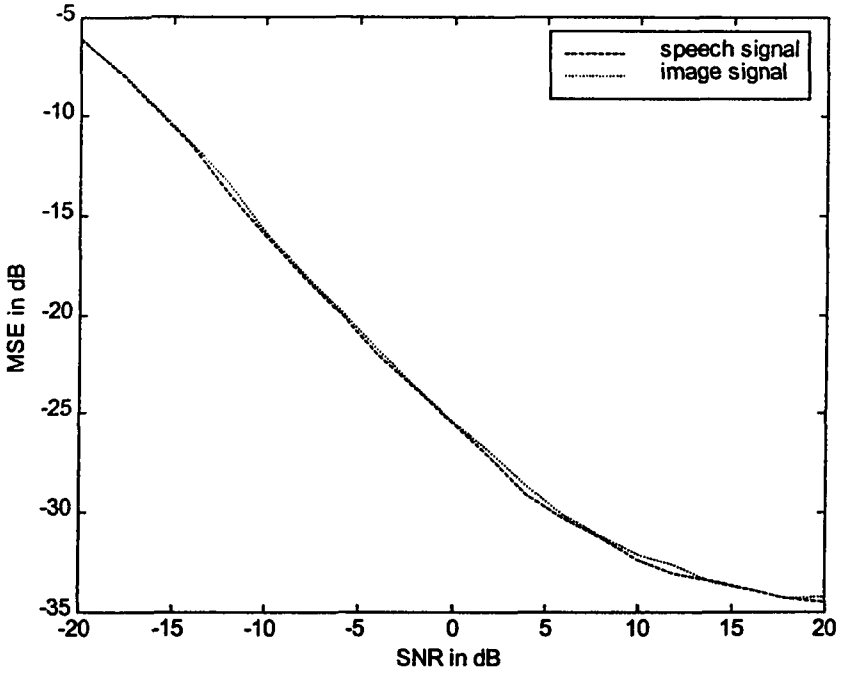

Figure 5.7. Signal recovery performance for speech and image signals.

5.4 Comparison with conventional SS digital communication systems

The analog ECPM approach is shown to be effective for practical SS analog communications. This scheme is suitable for the recent resurgence of interest in analog communication or partially analog approaches in the form of digital techniques [35]. Among the key reasons for considering analog communication techniques, a simpler motivation is that if an analog system can be used to achieve the performance of a digital system, its computation and implementation will be simpler compared to a fully digital approach. In this subsection, we will present the comparison of the performance between the proposed analog ECPM system with the conventional DSSS digital system.

In the standard DSSS digital system, as shown in Figure 1.1, the analog information signal should be scaled, quantized and converted to a binary sequence by a source coding process. To ensure the transmitted signal can be recovered under noise corruption, redundancy codes will be added through the channel coding process. The binary encoded signal is spread by multiplying with a long PN sequence. Then the modulated signal is transmitted after a RF modulation. At the receiver side, the RF

demodulated signal is despread by passing the coherent correlator, where it is multiplied with an identical PN sequence as that used in the transmitter. The detected binary signal is thereafter processed the channel error control decoding and the source dequantization steps. Thus the analog signal can be recovered. With the SS technique, the DSSS digital system can transmit the signal with a very small power but occupies broader bandwidth than the analog system.

Considering the difference of the analog ECPM and the digital DSSS systems, we employ a reasonable criterion to have a fair comparison. In our study, the energy per unit time period of the signal, denoted as E_s, is considered. It indicates that if we transmit a signal of a unit time period T_u, the energy used in both systems is fixed as the same. The performances of the analog ECPM and digital DSSS systems are evaluated by considering MSE performance versus the ratio of the E_s to the average power P_n of channel noise (E_sNR). That is,

$$E_sNR = \frac{E_s}{P_n} = \frac{1}{\delta_n^2}\int_0^{T_u} x^2(t)dt\,. \tag{5.10}$$

In our simulation, a random signal generated from a Gaussian process is used as the analog source. The generation rate is 1 kHz, and the unit time period T_u is 0.1 sec. Through the analog ECPM system, the signal will be modulated into the chaotic parameter as described in last subsection. For the DSSS digital system, the signal is sampled first by the sampling rate $f_s = 1\,kHz$. Each sampled symbol will be quantised. In our study, both 4-bits/symbol and 8-bits/symbol quantization levels are employed. The optimum qantizer is selected as the well-known Lloyd I algorithm [54,55]. In the first case, there is no channel error control coding employed, each quantised binary bit will be modulated directly by a long spreading codes (i.e. PN sequence) based on the BPSK modulation. The performances of both analog ECPM and digital DSSS are plotted in Figure 5.8. The x-axis is the E_sNR expressed in dB ranging between 20 to 80 dB with a step size of 5 dB. The y-axis represents the recovery distortion MSE expressed in dB.

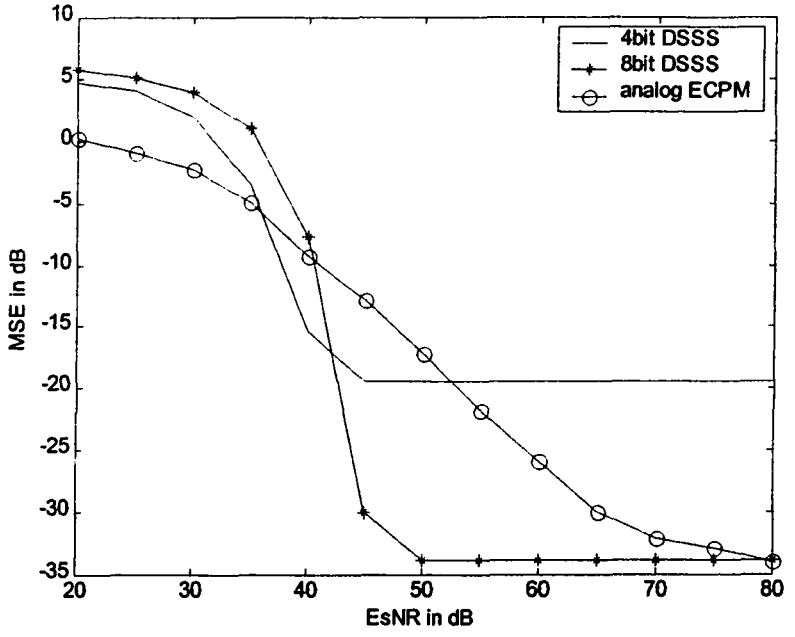

Figure 5.8. Comparison of analog ECPM system with conventional digital DSSS system, no error control coding is employed in the DSSS system.

From Figure 5.8, we observe that, in the range of $E_sNR > 45dB$, the recovery distortion performance MSE in the DS-SS digital communication system saturates for both 4-bits/symbol and 8-bits/symbol quantizations. At this transmission E_sNR level, the digital DSSS schemes are able to achieve a BER level of 0. In other words, there is no bit error occurred during the signal transmission and detection processes. The recovery distortion MSE comes from ADC and DAC processes. Distortion in the quantization of ADC and dequantization of DAC is inevitable in a digital communication system. In order to reduce this distortion, we can select a proper quantization scheme and increase the number of quantization level: R (bits/symbol). The relationship between distortion and quantization level is explained in the Shannon theorem: Source Coding with a Distortion Measure (1959a) [1]. The distortion measure function for a discrete-time memoryless Gaussian source due to a quantization process is given by:

$$Distortion = 2^{-2R}\delta_n^2. \tag{5.11}$$

Various quantization schemes have been proposed in literature and their distortion measure performances are plotted in Figure 5.9 [1]. From Figure 5.9, we observe that by increasing the quantization level R, the quantization distortion will be reduced. Therefore,

in Figure 5.8, at E_sNR >45dB, 8-bits/symbole quantization has a better performance than 4-bits/symbol quantization.

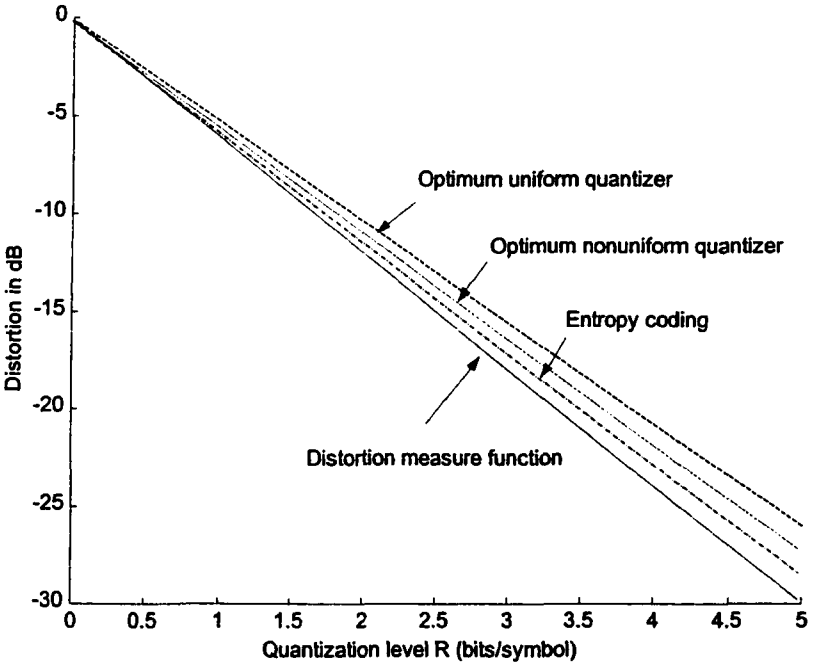

Figure 5.9. Distortion performance of various quantization schemes for discrete-time memoryless Gaussian source.

For E_sNR < 45dB, the channel noise is too high compared to the system transmission power. The receiver cannot achieve a perfect BER of 0, which means it cannot detect all the transmitted bits correctly. In this condition, if any transmitted binary bit is detected incorrectly, the demodulated symbol after the dequantization process will be totally wrong. This distortion is overwhelmingly large compared to the distortion introduced by ADC and DAC. The main recovery distortion MSE for the a digital system therefore depends on the BER performance for this E_sNR range. In general, the BER performance of a digital system is dependent of the ratio of the energy per bit E_b to the noise power density: E_bNR. For example, the BER performance of a standard DSSS scheme with BPSK modulation is given by the error probability function (Q-function) [1]:

$$P_e = Q\left(\sqrt{E_b NR}\right). \tag{5.12}$$

The relationship between the total energy E_s and the energy per bit E_b is given by:

$$E_s = N_s L E_b, \tag{5.13}$$

where N_s is the total samples of the transmitted signal and L denotes the number of encoded bits used to transmit one sample. In this case, if R bits/symbol quantization is used and no redundancy error control codes added, L=R. Combined Equation (5.10) and (5.11), the error probability function of the BER performance can be modified as:

$$P_e = Q\left(\sqrt{E_b NR}\right) = Q\left(\sqrt{\frac{E_s NR}{N_s L}}\right). \tag{5.14}$$

From the above equation, we observe that by fixing the E_sNR, when a higher bits/symbol rate R is used for quantization, the error probability will be increased, and hence results in an increase of the recovery distortion. Therefore, the performance of the 8 bits/symbol quantization scheme is worse than that of the 4 bits/symbol quantization scheme for E_sNR < 45dB.

From Figure 5.8, we observe that the performance of the analog ECPM system is much better than that of the digital scheme with 4-bits/symbol quantization at the range of $E_s NR < 37\ dB$ and $E_s NR > 52\ dB$. For $37\ dB < E_s NR < 52\ dB$, the ECPM is worse than 4-bits/symbol quantization. Compared with the performance of the digital scheme with 8-bits/symbol quantization at a low E_sNR level, say $E_s NR < 41\ dB$, the performance of ECPM is better. When the E_sNR becomes larger than 41 dB, the recovery distortion of the digital scheme is reduced at a faster rate (the slope of the MSE curve) than that of ECPM until it reaches its performance bound caused by the quantization. At around $E_s NR = 80\ dB$, the recovery performance of ECPM becomes almost the same as that of digital system with an 8-bits/symbol quantization.

Next, we consider the use of channel control coding in the digital system. The main purpose of the application of an error control coding scheme is that it can be used to detect and to correct bit errors that occur during message transmission in a digital communication system. Here, the linear block coding, Bose-Chaudhuri-Hocquenghem (BCH) code, is employed [56]. If each symbol is quantized into R bits previously through the source coding, then after error control coding, the total bits/symbol L in (5.14) is much larger than R. Usually, the BCH coding scheme is expressed as BCH(L,R). For the

4-bits/symbol quantization, BCH(7,4) coding is used. For the 8-bits/symbol quantization, BCH(127,8) is applied. It means that after adding the redundant codes, the total encoded bits/symbol is 7 and 127 respectively. The addition of redundant error control codes can correct certain detection errors during the transmission. However, if we fix the energy per signal within the unit time period, the longer bit length for one sample will also increase the total bit errors in (5.14). Therefore, the performance of the digital scheme is not improved significantly by adding the error control coding scheme, as shown in Figure 5.10. The relationship of the performances of the digital DSSS and analog ECPM systems remains the same.

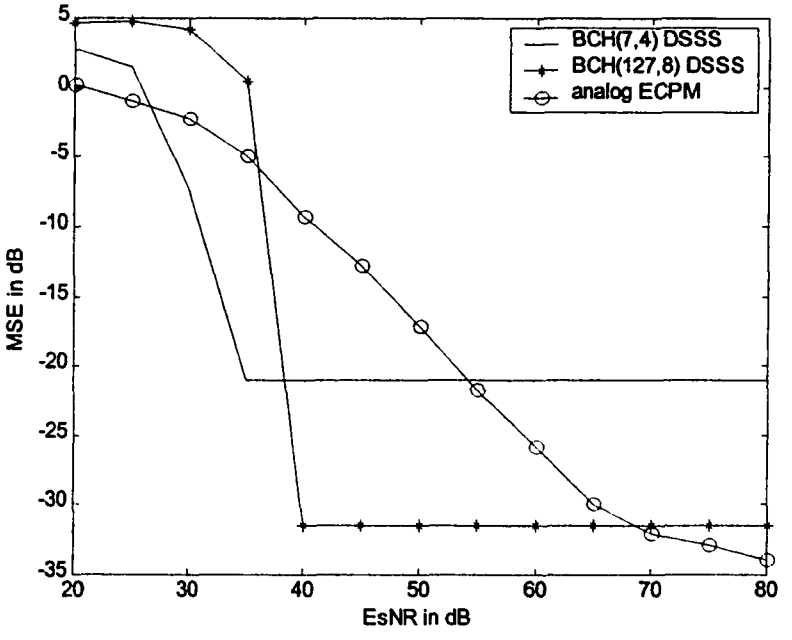

Figure 5.10. Comparison of analog ECPM system with conventional digital DSSS system, BCH error control coding is employed in the DSSS system.

Overall speaking, we found the performance of the ECPM SS analog communication system cannot outperform the conventional SS digital communication system for all the transmission condition E_sNR. However, its performance is already very closed to the digital scheme. In addition, unlike the digital scheme, which has inevitable quantization distortion, its performance can still be improved. If we consider its other advantages, such as simple structure, without quantization and coding schemes, without

synchronization, etc, the analog ECPM communication system is still a good choice for the perspective SS communications [57].

CHAPTER 6

CONCLUSIONS

In this thesis, we develop a novel method based on the ergodic property of chaotic signals for estimating the bifurcating parameter of a chaotic signal in noise. The proposed method is shown to work effectively even in a very low SNR environment. It is also shown that the proposed method significantly outperforms other conventional techniques in terms of estimation accuracy. In addition, the proposed method is very simple in terms of computational complexity. The main drawback of the proposed method is that it cannot be applied to any chaotic system in general. Only those have a monotone mean value function over the parameter range of consideration can take advantage of this efficient estimation technique. However, the proposed technique is still valuable. First, it shows that the parameters of chaotic signals can indeed be estimated accurately in a low SNR environment, which is a question that has bothered many chaotic signal processing researchers for a long time. Second, the proposed method can be used in many applications where the chaotic systems can be chosen by the system designer. And one of such applications is the chaotic spread spectrum communications.

Based on this novel ergodic estimation concept, a new SS communication scheme called the ergodic chaotic parameter modulation (ECPM) is developed. Not only does this new ECPM communication system not require any synchronization procedure, but it also has an extremely simple structure for implementation. In fact, its demodulator is even much simpler than the standard correlator. Although ECPM is a non-coherent scheme, it is shown that it is superior to all other conventional chaotic communication methods in terms of bit error rate performance. In fact, if the noise mean can be estimated accurately, the BER performance of the ECPM SS system is found to be almost perfect.

For comparison, the proposed ECPM system and several most popular chaos based digital communication schemes to-date are investigated thoroughly. Apart from the common advantages of infinite sequences, aperiodicity and high security, the performances of these chaos-based communication systems are evaluated under different communication conditions, including noise performance in an AWGN channel, the effect

of data rate, synchronization error and multipath channel. The CSS and CC offer alternative spreading sequence (or carrier) for the conventional DSSS system to spread the information data, their performances are therefore almost identical to that of DSSS. For other chaos based communication schemes, only ECPM and FM-DCSK can achieve a comparative BER performance with that of DSSS in an AWGN channel. However, most of chaos based communication systems show improved robustness performance in various communication conditions to some extent. For example, FM-DCSK shows strong robustness against the higher data rate. Both ECPM and FM-DCSK can operate well through mulitpath channel as well as those DSSS based systems: CSS and CC. Some of these chaos modulation schemes including ECPM, CM and AF-CPM are very robust to the synchronization error. Overall speaking, ECPM is found to have the best performance in terms of both noise behaviour and robustness. Because of the robustness of chaotic modulation communication scheme, they are suitable for lots of potential communication applications in a complicated environment.

In addition to digital communication, the mean value estimation technique can be also applied to SS analog communications. The analog ECPM system can transmit and recover an analog signal, such as sinusoidal signal, random signal, speech and images, without any quantization and coding as required in a digital scheme. The analog signal can be transmitted with a very low signal power but achieve a great performance. By comparing with the conventional DSSS system, its performance is still worse than that of the digital schemes under certain E_sNR level. However, the performance of the analog ECPM system is already comparable to that of digital schemes. A major advantage of analog ECPM system is that it doesn't require ADC and DAC processes, which makes its structure and computing workload simpler. The nature of its analog transmission offers it lots of potential in the perspective applications of SS technique, such as SS walky-talky, SS cordless phone, wireless home network, etc.

The abilities for digital and analog implementations with well performance make the proposed ECPM system superior to other chaotic communication schemes. Our future research works focus on the improvement of the performance of the ECPM scheme for both digital and analog transmission. A real system will be established for practical RF applications.

REFERENCES

[1] Proakis J.G., *Digital Communications*, Third Edition, McGraw-Hill Inc, 1998.

[2] Cooper G.R. and C.D. McGillem, *Modern Communications and Spread Spectrum*, McGraw-Hill Book Company, 1986.

[3] Dixon R.C. *Spread Spectrum Systems with Commercial Applications*, 3rd ed. New York: Wiley, 1994.

[4] Boyarsky A. and P. Gora, *Laws of Chaos: Invariant Measures and Dynamical Systems in One Dimension*, Birkhauser, Boston/Basel/Berlin, 1997.

[5] Parker T.S. and L.O. Chua, *Practical Numerical Algorithms for Chaotic Systems*, Springer-Verlag, New York, 1989.

[6] Kennedy M.P., R. Rovatti and G. Setti, *Chaotic Electronics in Telecommunications*, CRC Press, 2000.

[7] Itoh M. "Spread spectrum communication via chaos," *International Journal of Bifurcation and Chaos*, vol. 9, no. 1, pp. 155-213, 1999.

[8] Kennedy M.P. and G. Kolumban, "Digital communications using chaos," *Signal Processing* 80 (2000), pp.1307-1320, 2000.

[9] Yu H. and H. Leung, "A comparative study of different chaos based spread spectrum communication systems," *Proceedings of IEEE ISCAS*, vol. 3, pp.213-216, Sydney, Australia, May 2001.

[10] Umeno K. and K. Kitayama "Spreading sequences using periodic orbits of chaos for CDMA," *Electronics Letters*, vol.35 no.7, pp.545-546, 1999.

[11] Mazzini G., G. Setti and R. Povatti, "Chaotic complex spreading sequences for asynchronous DS-CDMA-Part I: system modeling and results," *IEEE Transactions on Circuits and Systems-I: Fundamental Theory and Applications*. vol. 44, no.10, pp.937-947, 1997.

[12] Heidari-Bateni G. and C.D. McGillem, "A chaotic direct-sequence spread spectrum communication system," *IEEE Transactions on Communications*, vol.42, no. 2, pp. 1524-1527, 1994.

[13] Yang T. and L.O. Chua, "Chaotic digital code division multiple access (CDMA) communication systems," *International Journal of Bifurcation and Chaos*, vol.7, no.12, pp.2789-2805, 1997.

[14] Yang T. and L.O. Chua, "Applications of chaotic digital code-division multiple access (CDMA) to cable communication systems," *International Journal of Bifurcation and Chaos*, vol.8, no.8, pp.1657-1669, 1998.

[15] Kolumban G., G. Kis, Z. Jako, and M.P. Kennedy, "FM-DCSK: A robust modulation scheme for chaotic communications, " *IEICE Trans. Fundamentals of Electronics, communications and Computer Sciences,* E81-A(9), pp.1798-1802, 1998.

[16] Kennedy M.P., G. Kolumban, G, Kis and Z. Jako, "Performance evaluation of FM-DCSK modulation in multipath environments," *IEEE Transactions on Circuits and Systems-I: Fundamental Theory and Applications*. vol. 47, no.12, pp.1702-1711, 2000.

[17] Elmirghani J.M.H. and R.A. Cryan, "Communication using chaotic masking," *IEE Colloquium on Exploiting Chaos in Signal Processing*, pp. 12/1-12/6, 1994.

[18] Chen Y.-Y., "Masking messages in chaos," *Europhysics Letters*, vol. 34, pp.245-250, May, 1996.

[19] Kennedy M.P., H. Dedieu, and M. Hasler, "Chaos shift keying: modulation and demodulation of a chaotic carrier using self-synchronizing Chua's circuits," *IEEE Trans. Circuits and Systems - II*, vol. 40, no. 10, pp. 634-642, 1993.

[20] Kolumban G., M.P. Kennedy and L.O. Chua, "The role of synchronization in digital communications using chaos-part II: chaotic modulation and chaotic synchronization", *IEEE Transactions on Circuits and Systems-I: Fundamental Theory and Applications*. vol. 45, no.11, pp.1129-1139, 1998.

[21] Kocarev L., K.S Halle, K. Eckert, L.O. Chua's, and U. Parlitz, "Experimental demonstration of secure communications via chaotic synchronization," *International Journal of Bifurcation and Chaos*, vol. 2, no. 3, pp. 709-713, 1992.

[22] Leung H. and J. Lam, "Design of demodulator for the chaotic modulation communication system," *IEEE Transactions on Circuits And Systems-I: Fundamental Theory And Applications*, vol.44, no.3, pp.262-267, 1997.

[23] Zhu Z. and H. Leung, "Adaptive identification of nonlinear systems with application to chaotic communications," *IEEE Transactions on Circuits and Systems-I: Fundamental Theory and Applications*. vol. 47, no. 7, pp.1072-1080, 2000.

[24] Leung H. and X. Huang, "Parameter estimation in chaotic noise," *IEEE Transactions on Signal Processing*, vol.44, no.10, pp.2456-2463, 1996.

[25] Chan A.M. and H. Leung, "Equalization of speech and audio signals using a nonlinear dynamical approach," *IEEE Transactions on Speech and Audio Processing*, vol.7, no.3, pp.356-360, 1999.

[26] Leung H., "System identification using chaos with application to equalization of a chaotic modulation system," *IEEE Transactions on Circuits and Systems* - I, vol.45, no.3, pp.314-320, 1998.

[27] Fu Y. and H. Leung, "Narrowband interference cancellation in a spread spectrum system using chaos," accepted for publication in *IEEE Transactions on Circuits and Systems –I.*

[28] Kostelich E.J., "Noise reduction in chaotic time series data: A survey of common methods," *Physical Review E*, vol.48, no.3, pp.1752-1763, 1993.

[29] Weigend A.S. and N.A. Gershenfeld, editors, *Time Series Prediction: Forecasting the Future and Understanding the Past*, Santa Fe Institute, Studies in the Sciences of Complexity, Addison-Wesley 1994.

[30] Kay S.M., "Methods for chaotic signal estimation," *IEEE Transactions on Signal Processing*, vol.43, no.8, pp.2013-2016, 1995.

[31] Wang S., P.C. Yip and H. Leung, "Estimating initial conditions of noisy chaotic signals generated by piecewise linear Markov maps using itineraries," *IEEE Transactions on Signal Processing*. vol. 47, no.12, pp. 3289-3302, 1999.

[32] Pantaleon C., D. Luengo and I. Santamaria, "Optimal estimation of chaotic signals generated by piecewise linear maps," *IEEE Signal Processing Letters*, vol.7, no.8, pp.235-237, 2000.

[33] Parodi G., S. Ridella and R. Zunions, "Using chaos to generate keys for associative noise-like coding memories," *Neural Networks*, vol.6, pp.559-572, 1993.

[34] Papadimitriou S., A. Bezerianos and T. Bountis, "Secure communication with chaotic systems of difference equations," *IEEE Transactions on Computer*, vol.46, no.1, pp.27-38, 1997.

[35] Chen B. and G.W. Wornell, "Analog error correcting codes based on chaotic dynamical systems," *IEEE Transactions on Communications* vol. 46, no.7, pp.881-890, 1998.

[36] Isabelle S.H. and G.W. Wornell, "Statistical analysis and spectral estimation techniques for one dimensional chaotic signals," *IEEE Transactions on Signal Processing*, vol.45, no.6, pp.1495-1506, 1997.

[37] Kohda T. and A. Tsuueda, "Statistics of chaotic binary sequence," *IEEE Transactions on Information Theory*, vol. 43, no, 1, pp. 104-112, 1997.

[38] Kohda T. and A. Tsuueda and A.J. Lawrance, "Correlational properties of Chebyshev chaotic sequences," *Journal of Time Series Analysis*, vol. 21, no. 2, pp. 181-192, 2000.

[39] Ott E., T. Saucer and J.A. Yorke, *Coping with Chaos: Analysis of Chaotic Data and the Exploitation of Chaotic Systems*, John Wiley & Sons, New York/Chichester, 1994.

[40] Haykin S., *Adaptive Filter Theory*, 2nd Edition, Prentice Hall, 1991.

[41] Ueberhuber C.W., *Numerical Computation 2: Methods, Software and Analysis*, Springer-Verlag: Berlin Heidelberg, 1997.

[42] Boyarsky A. and M. Scarowsky, "On a class of transformations which have unique absolutely continuous invariant measures," *Transactions of American Mathematical Society*, vol.255, no.11, pp.243-262, 1979.

[43] Jeruchim M.C., P. Balaban and K.S. Shanmugan, *Simulation of Communication Systems*, Plenum Press, New York and London, 1992.

[44] Leung H., H. Yu and S. Wang, "Estimation of chaotic parameters in low SNR with applications to chaotic communications," submitted to *IEEE Transactions on Circuits and Systems-I: Fundamental Theory and Applications.*

[45] Abel A., W. Schwarz and M. Gotz, "Noise performance of chaotic communication systems," *IEEE Transactions on Circuits and Systems-I: Fundamental Theory and Applications*. vol. 47, no. 12, pp.1726-1732, 2000

[46] Kolumban G., "Theoretical noise performance of correlator-based chaotic communication schemes," *IEEE Transactions on Circuits and Systems-I: Fundamental Theory and Applications*. vol. 47, no. 12, pp.000-000, 2000

[47] Chen C.C. and K. Yao, "Numerical Evaluation of Error Probabilities of Self-Synchronizing Chaotic Communications," *IEEE Communications Letters*, vol. 4, no. 2, pp. 37-39, 2000.

[48] Simon M.K., J.K. Omura, R.A. Scholtz and B.K. Levitt, *Spread Spectrum Communications Handbook,* revised edition, McGraw-Hill, Inc, New York, 1994.

[49] Rappaport T.S., *Wireless Communications: Principles and Practice*, Prentice Hall PTR, 1996.

[50] Leung H. and T. Lo, "Chaotic radar signal processing over the sea," *IEEE Transactions on Oceanic Engineering,* vol.18, no.3, pp.287-295, 1993.

[51] Chow P.E.-K., "Performance in waveform quantization," *IEEE Transactions on Communications*, vol.40, Nov, pp. 1737 –1745, 1992.

[52] Ouvry L., C. Boulanger and J.R. Lequepeys, "Quantization effects on a DS-CDMA signal," *1998 IEEE 5th International Symposium on Spread Spectrum Techniques and Applications*, vol. 1, pp. 234-238, September, 1998.

[53] Abuelma'atti M.T., "Effect of bit-threshold errors on the harmonic and intermodulation performance of successive approximation A/D converters," *IEEE Transactions on Communications*, vol.41, No.8, August, pp. 1155-1160, 1993.

[54] Lloyd S.P., "Least squares quantization in PCM," *IEEE Transactions on Information Theory*, vol. IT-28, pp.129-137, March, 1982.

[55] Gersho A. and R.M. Gray, *Vector Quantization and Signal Compression*, Kluwer academic publishers, Boston, MA, 1991.

[56] Wang W., *Communications Toolbox: For Use With MATLAB*, The Math Works. Inc, Natick MA, 1996.

[57] Hassan A.A., J.E. Hershey and G.J. Saulnier, *Perspectives in Spread Spectrum*, Kluwer Academic Publishers, Boston/Dordrecht/London, 1998.